A COMPUTATIONAL APPROACH FOR **DESIGNING** TRIP STEELs **STUDYING**

Shengyen Li

Shengyen.li@nist.gov

June 2, 2014

Alloy Design

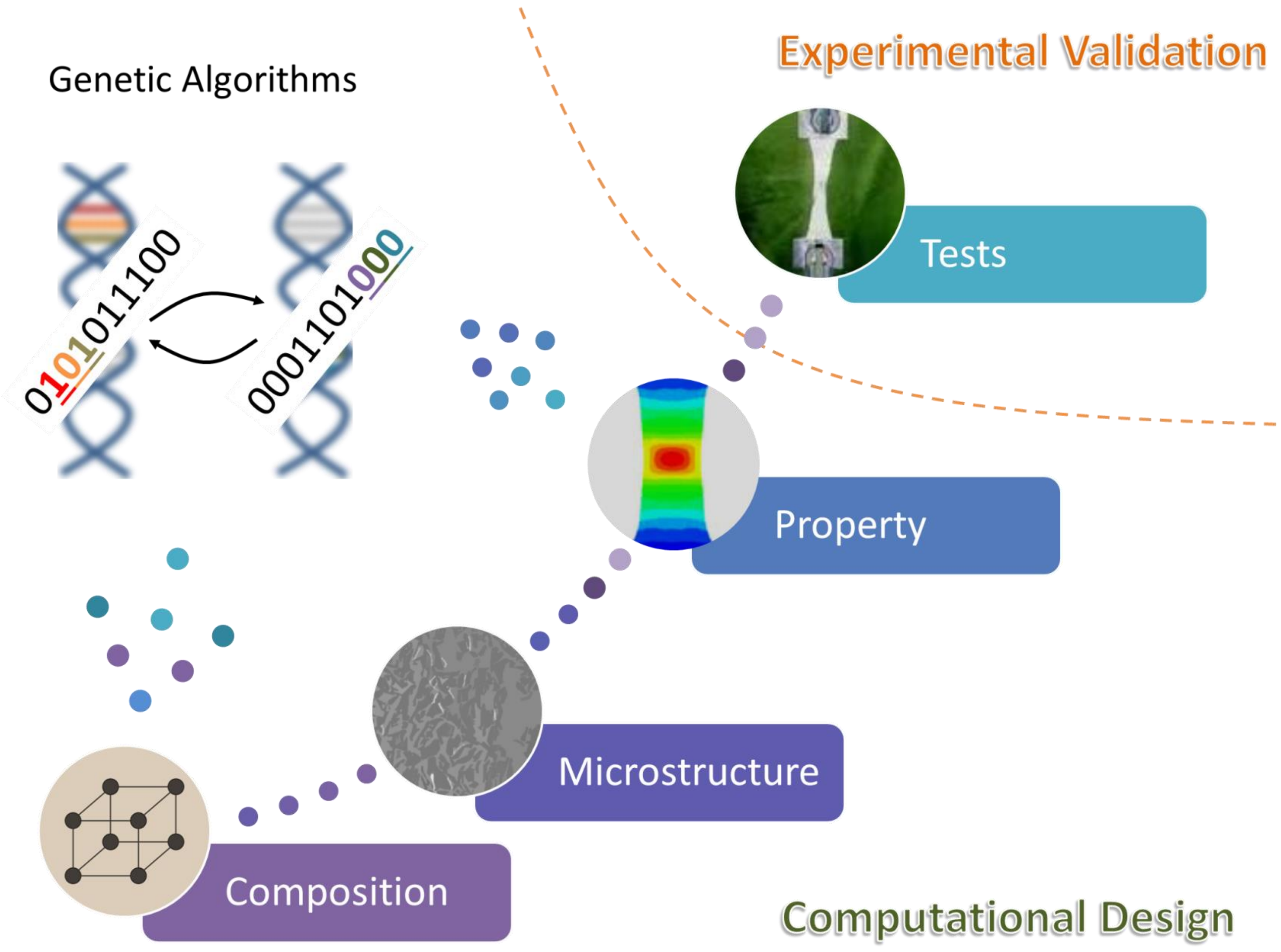

Experimental Results - Fe-0.32C-1.42Mn-1.56Si

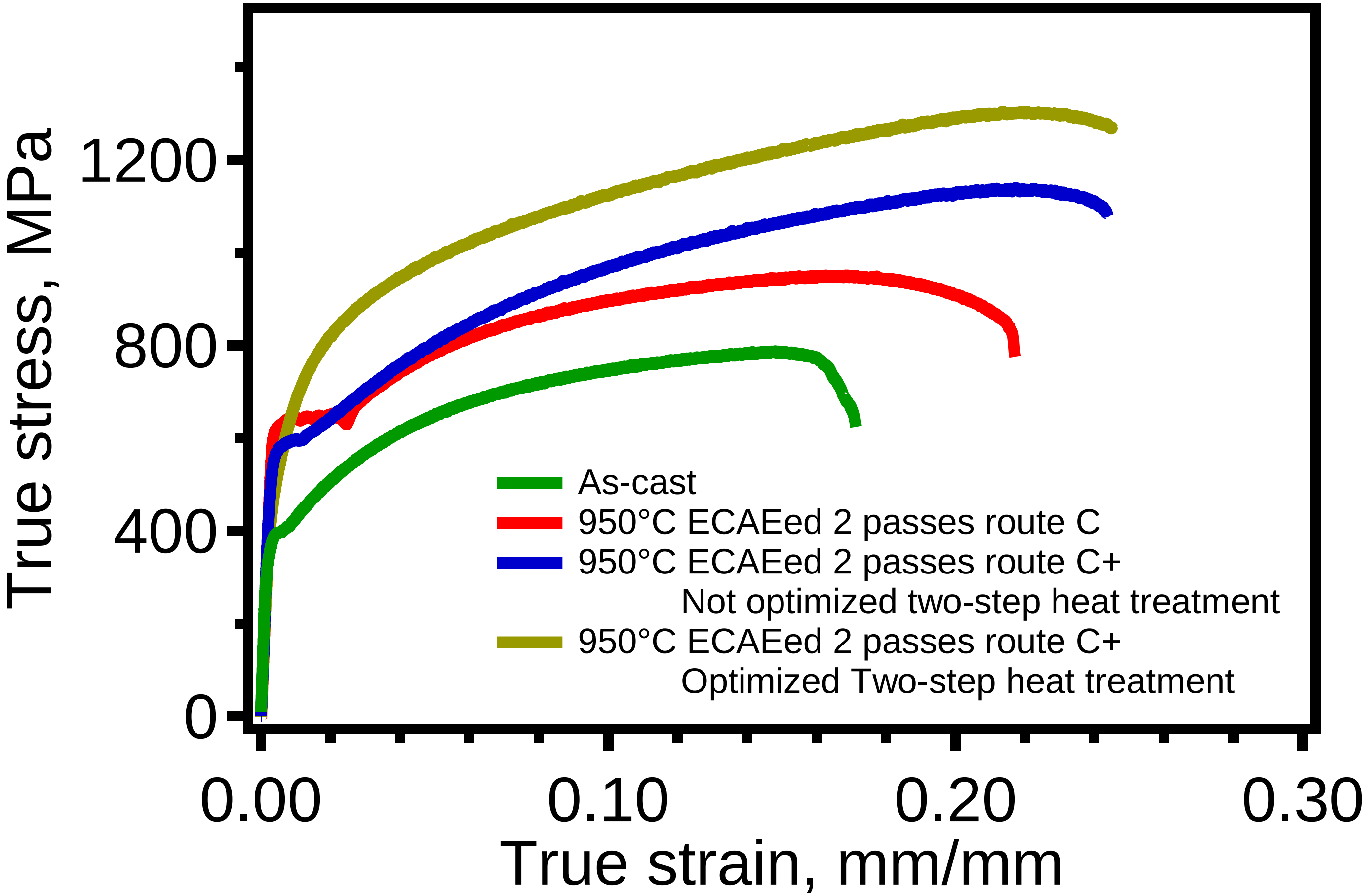

Outline

- Motivations
- CALPHAD-based Models
- Mechanical Models
  - Swift Model
  - Irreversible Thermodynamics
- Genetic Algorithms
- Artificial Neural Network
- Conclusion

The Properties of TRIP Steel

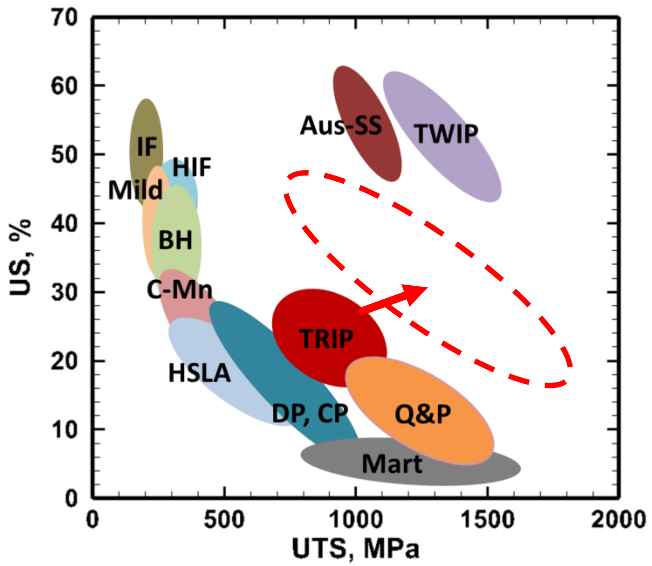

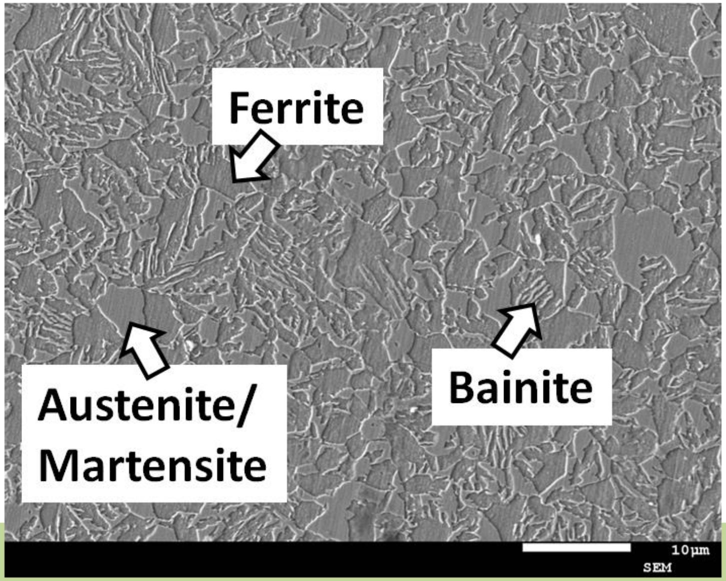

Why TRIP Steel

- Transformation Induced Plasticity
- Martensitic transformation during plastic deformation contributes to overall ductility

How to make TRIP steels

- Select chemical composition properly
- Apply **two-step** heat treatment to manage the carbon content in austenite

Target

- Maximize **TRIP effect** of the **low alloying addition** TRIP steel

Key

- Stabilize austenite against the martensitic transformation during heat treatment
- Suppress the formation of cementite

Zhu, Acta Mat., 2012

Two-Step Heat Treatment

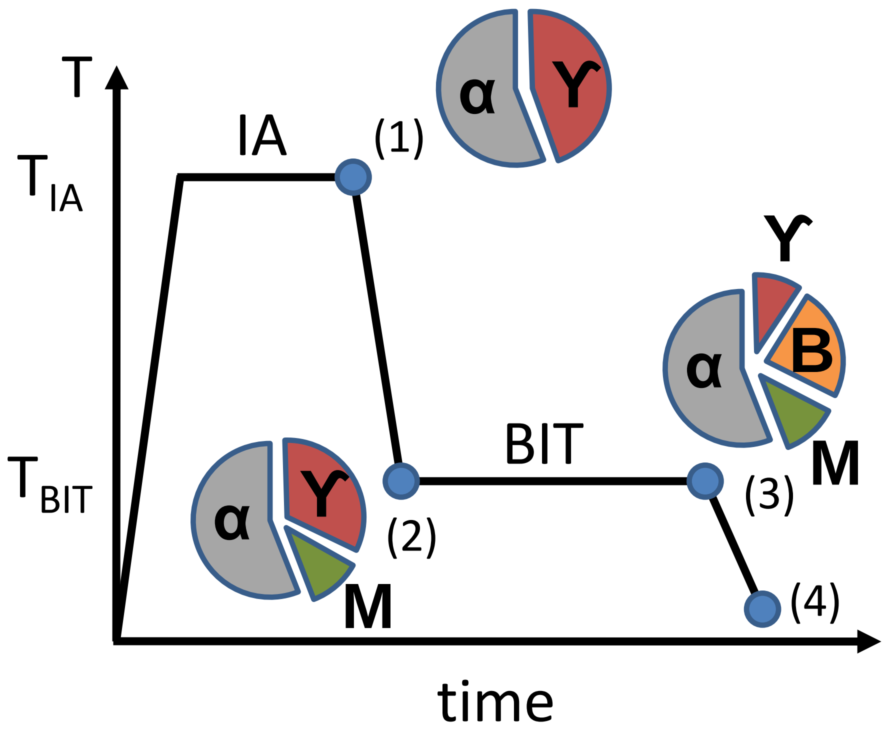

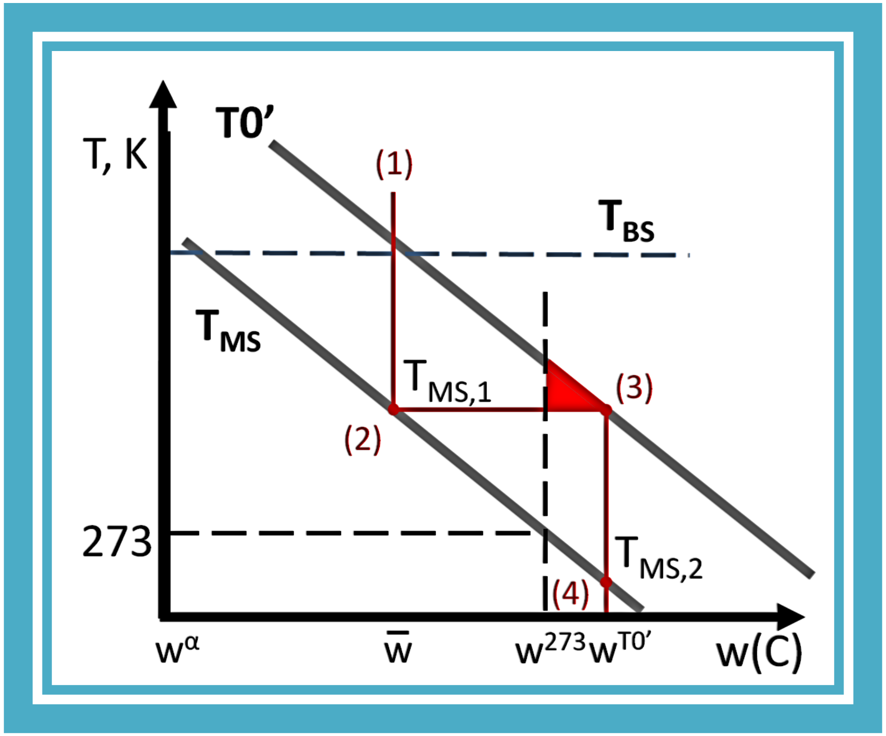

Two-step heat treatment: (1) inter-critical annealing (IA) (2)-(3) bainite isothermal transformation (BIT) (3)-(4) final cooling to room temperature

Two-Step Heat Treatment

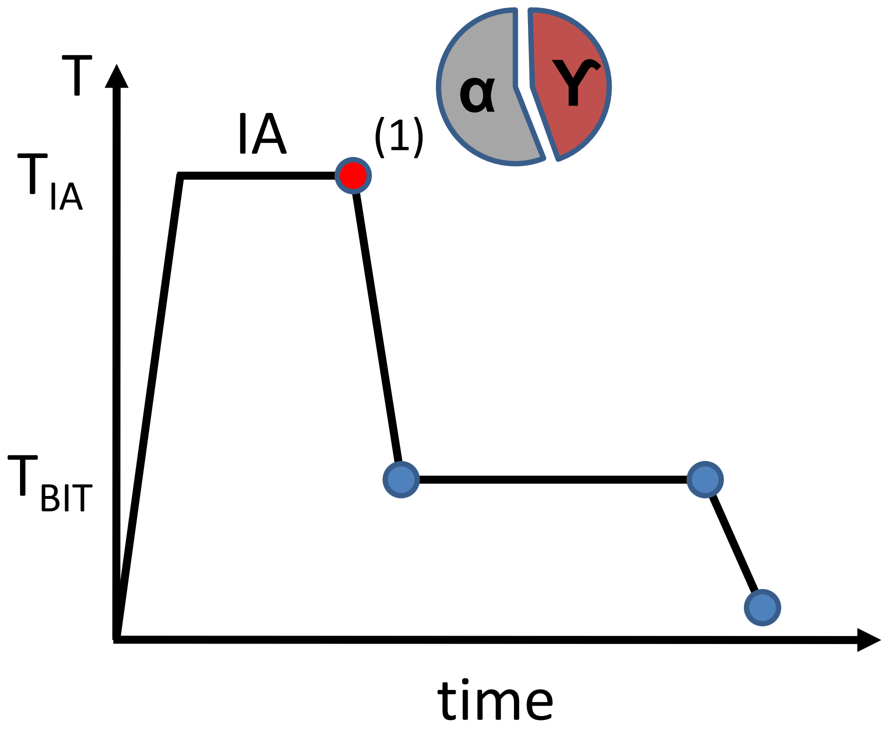

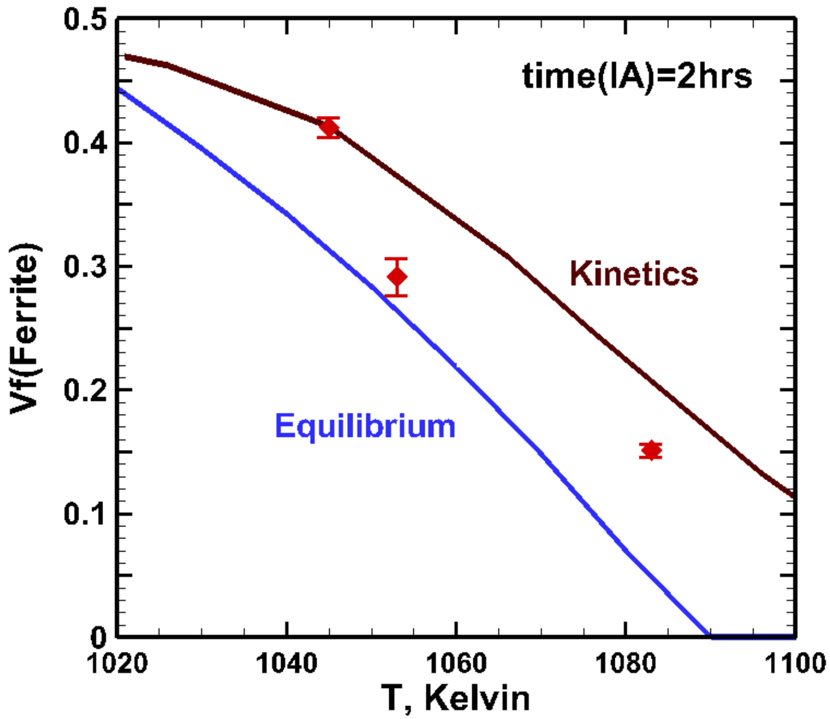

Two-step heat treatment: (1) inter-critical annealing (IA)

Two-Step Heat Treatment

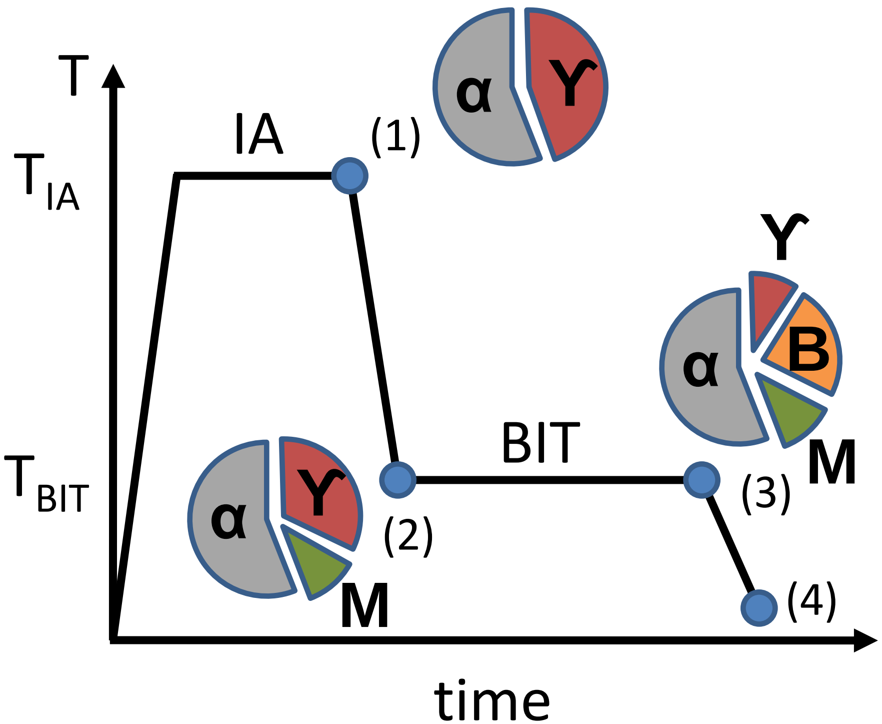

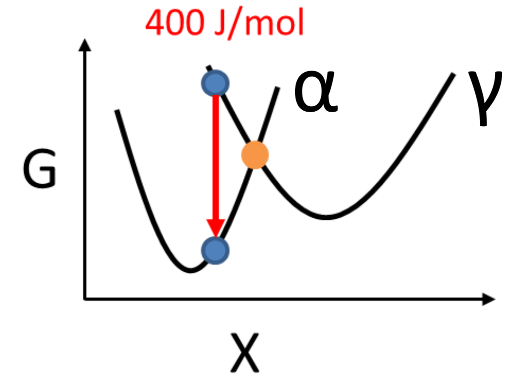

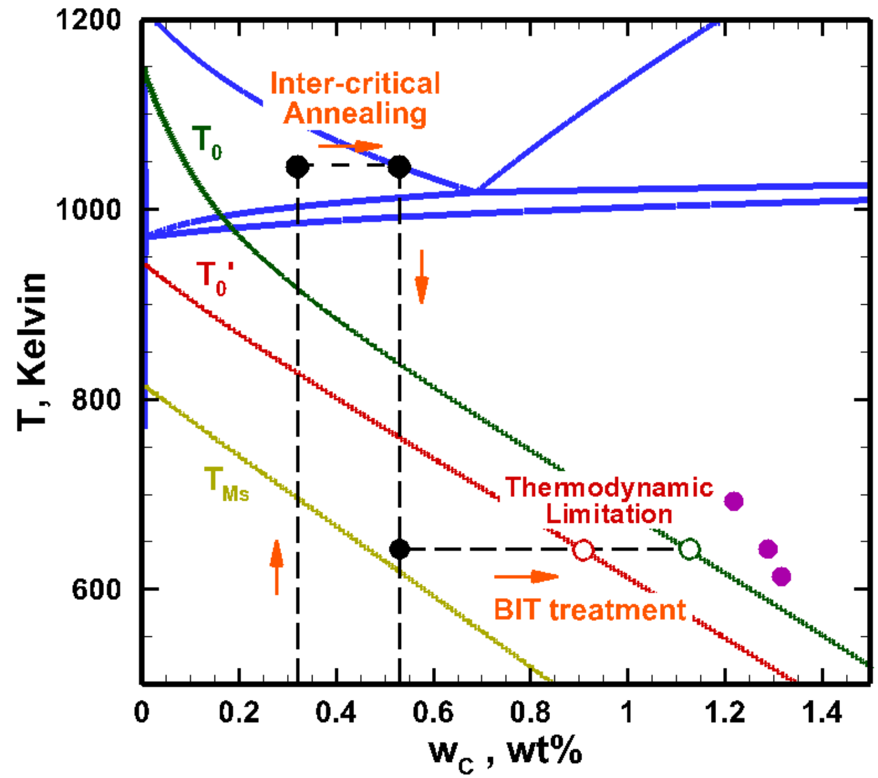

Two-step heat treatment: (1) inter-critical annealing (IA) (2)-(3) bainite isothermal transformation (BIT) (3)-(4) final cooling to room temperature

Li, Acta Mat., 2012
Li, Acta Mat., 2013

Displacive Bainitic Transformation

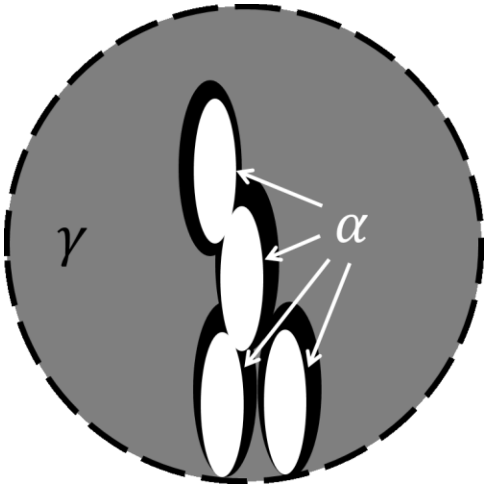

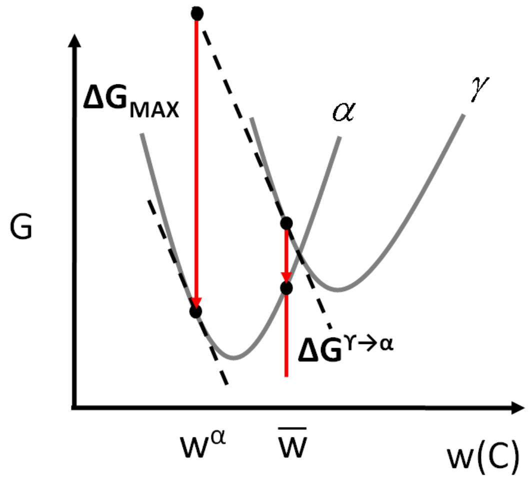

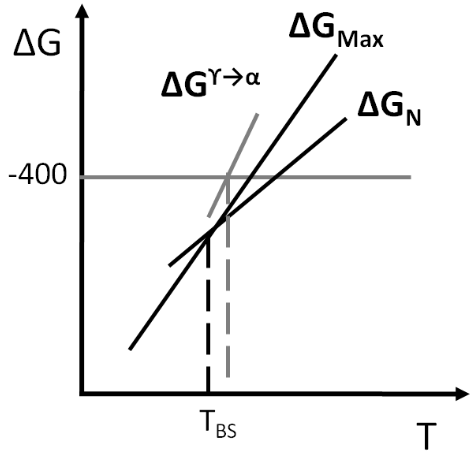

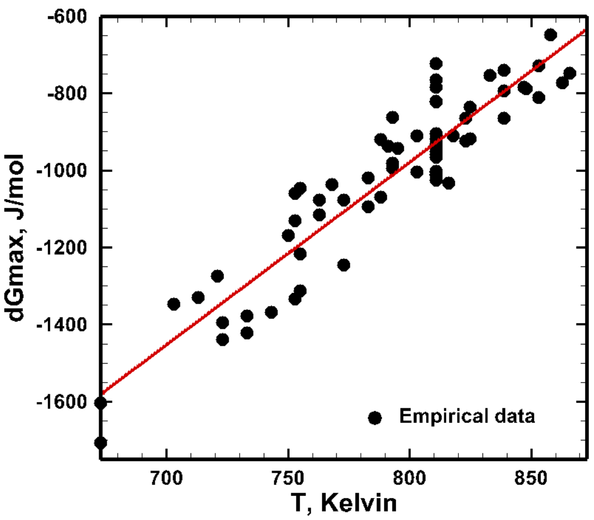

- The Gibbs free energies of bainitic ferrite and austenite are equal at T_0.
- 400 J/mole of the strain energy is considered for bainitic transformation as T_0'.
- The non-homogeneous C-distribution sustains the bainitic transformation.
- The curve is fitting based on database TCFE6 V6.2
- The empirical data is obtained from: Chang et al., Met. Mat. Tran. A, 1999 and Zhao et al., J. Mat. Sci., 2001

Heterogeneous Carbon Distribution

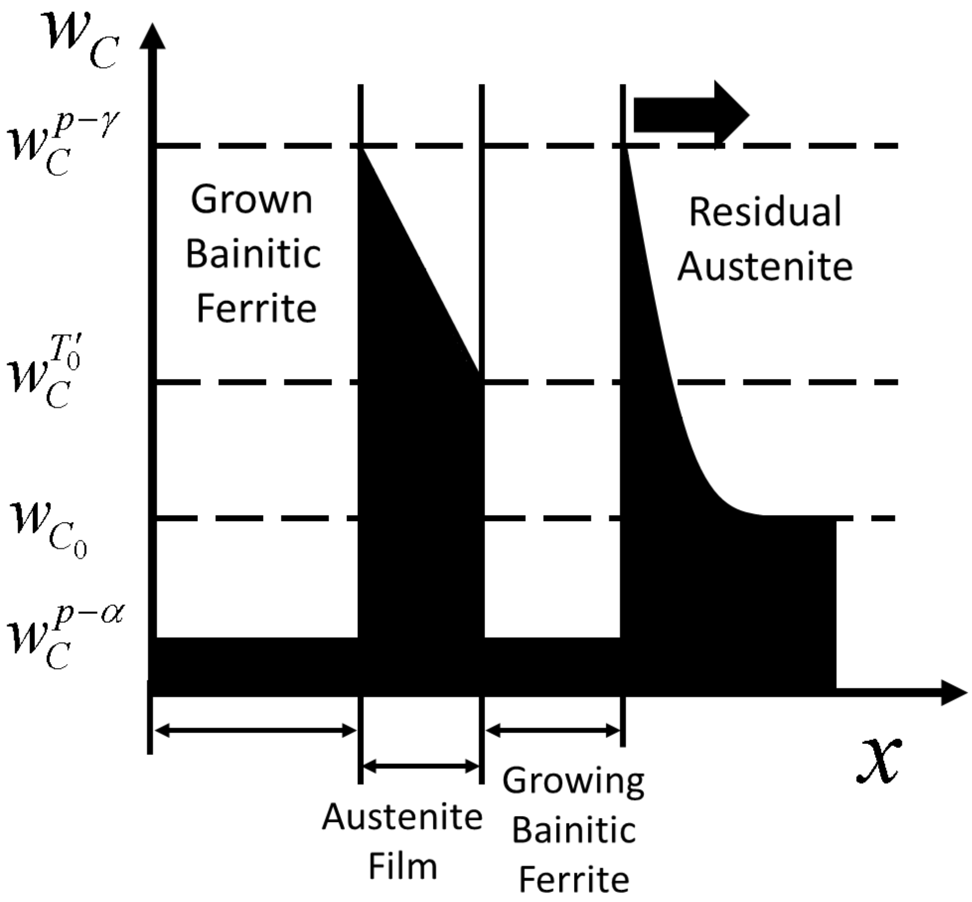

"During the growth some carbon diffuses out of the ferrite grains into the surrounding austenite matrix. The higher the temperature of formation, the freer the ferrite is of supersaturated carbon."

– Zener, 1912

Heterogeneous Carbon Distribution (1)

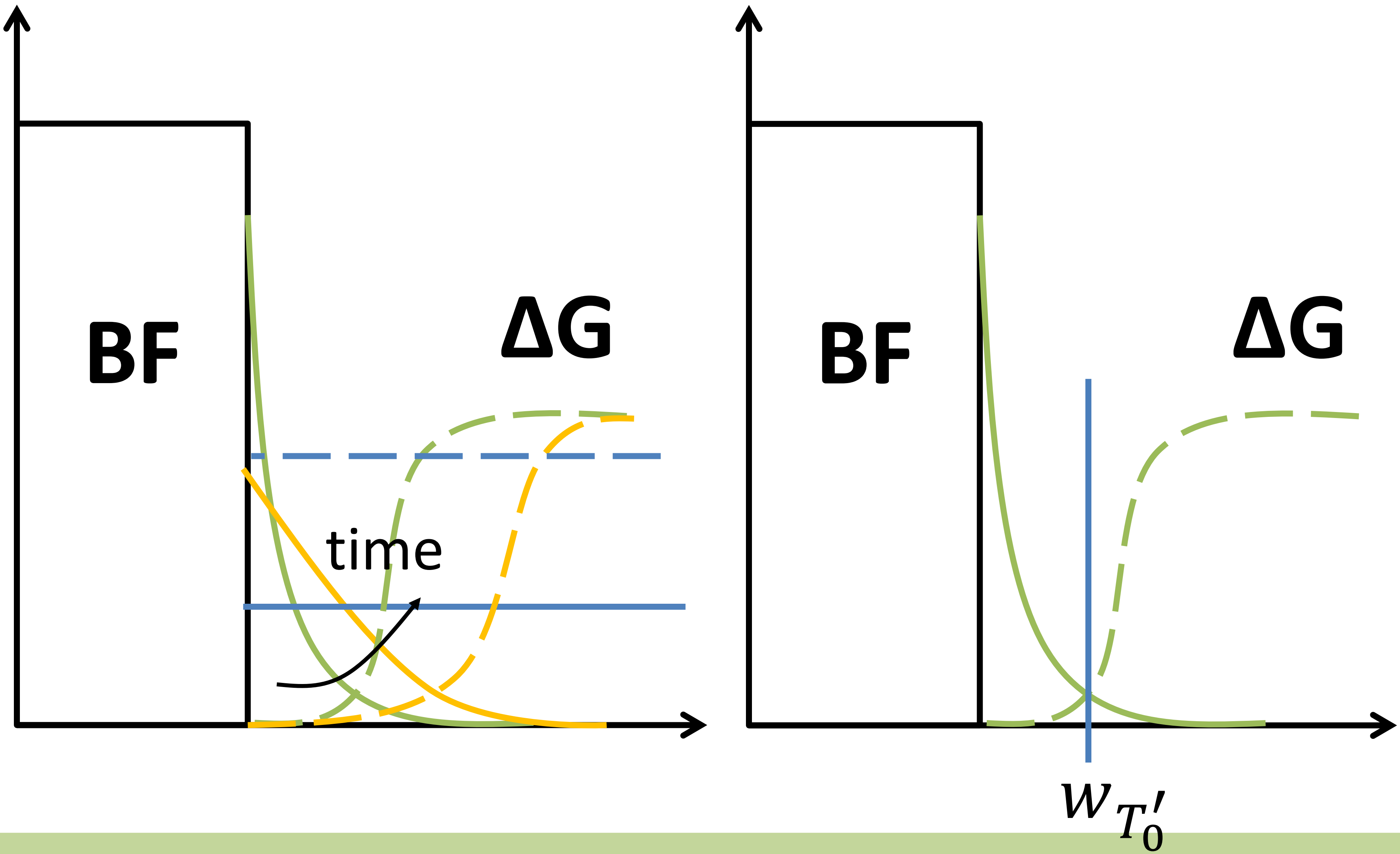

Heterogeneous Carbon Distribution (2)

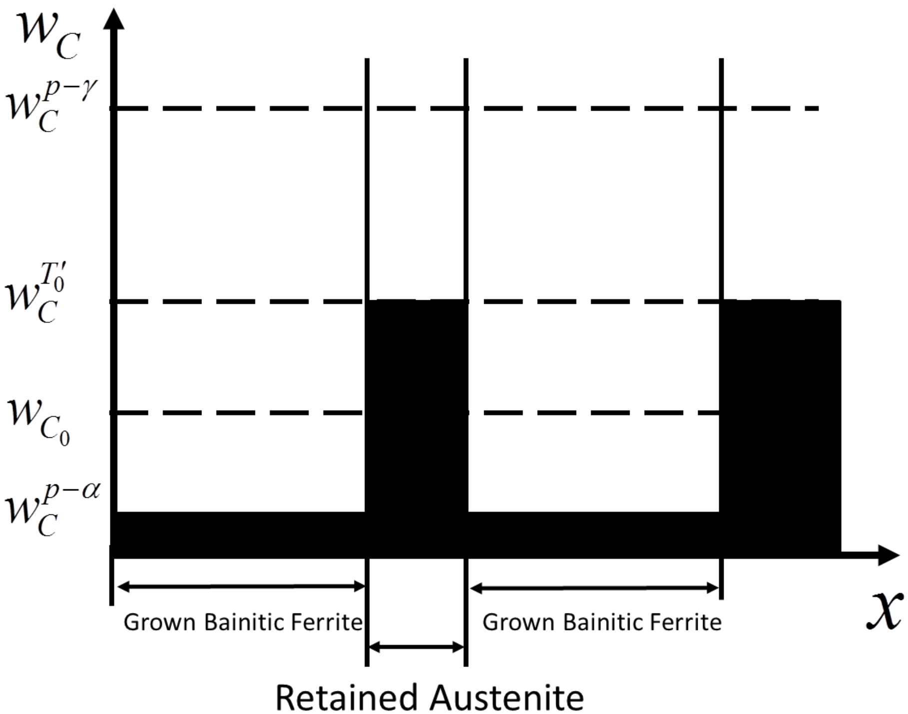

DC >> df

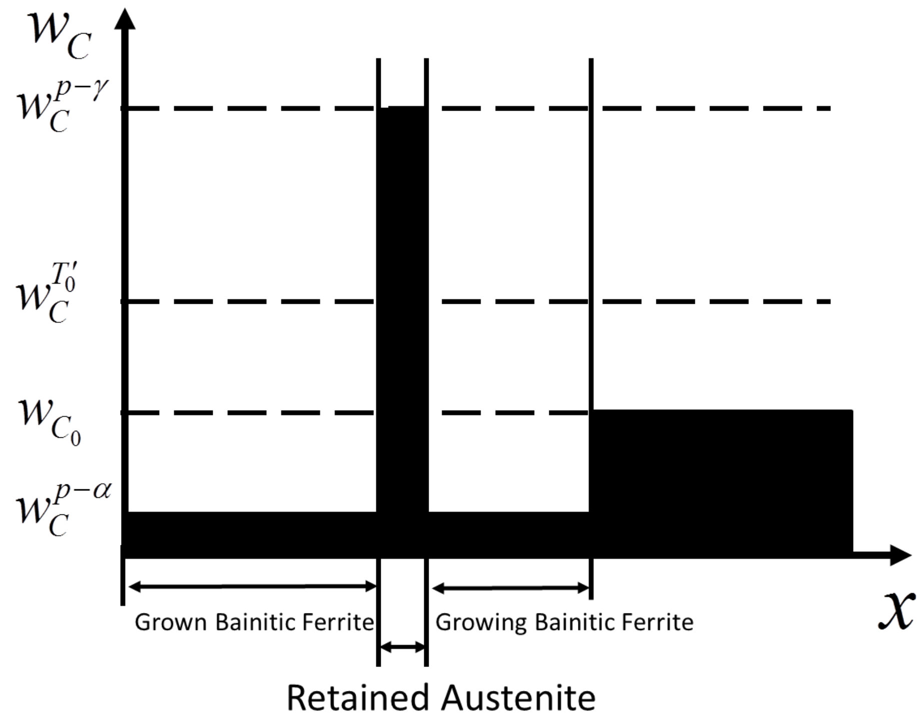

DC << df

Heterogeneous Carbon Distribution (3)

Caballero et al., 2011

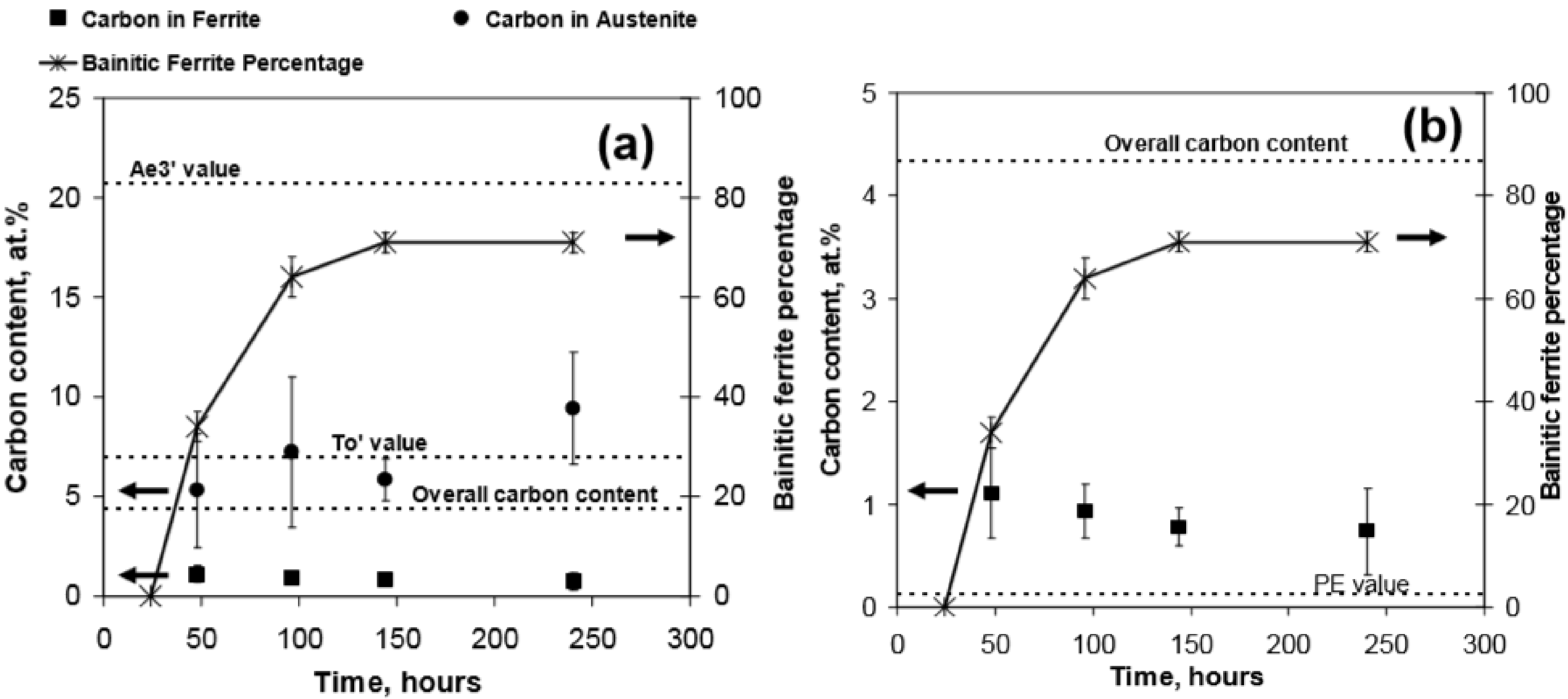

Two-Step Heat Treatment

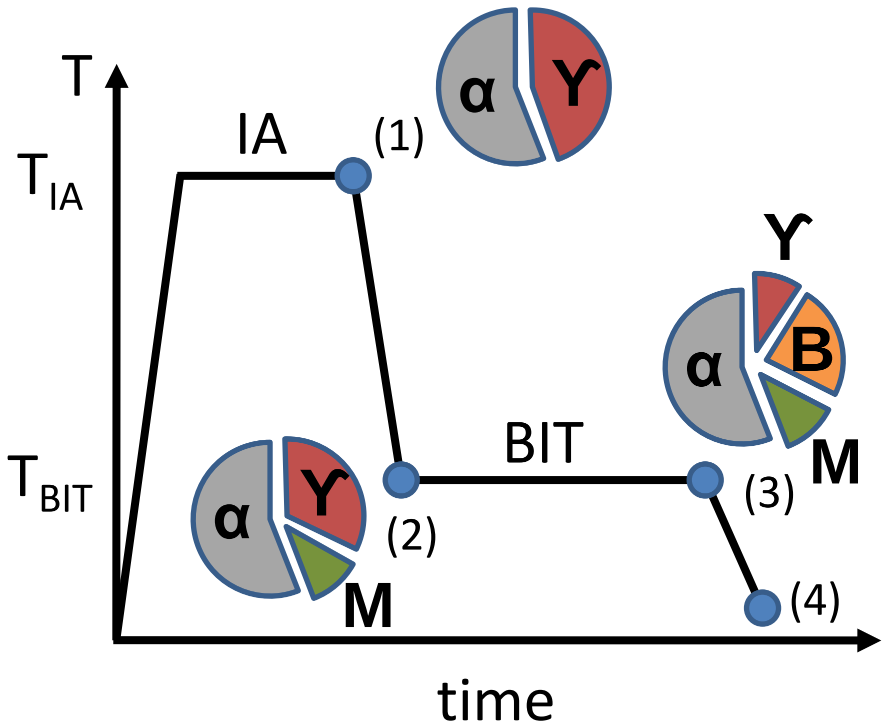

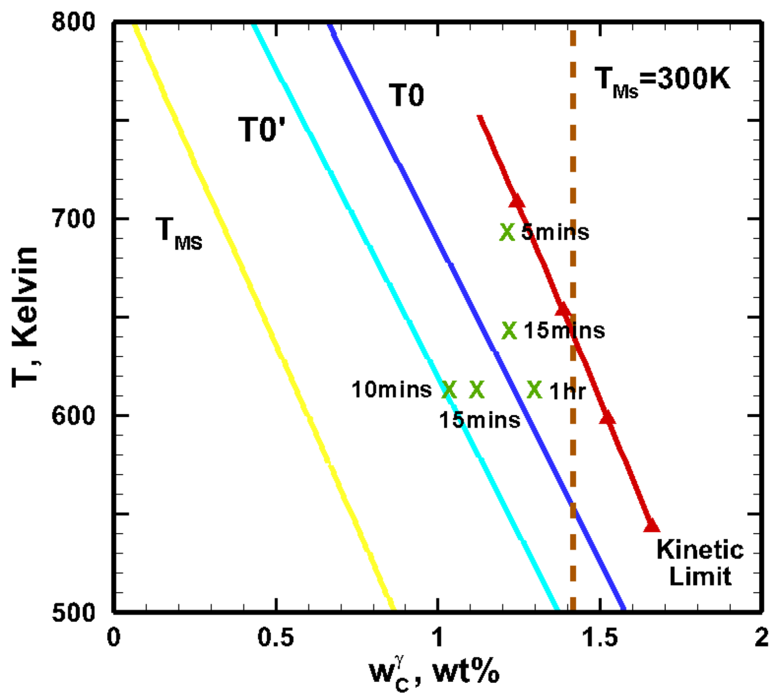

Two-step heat treatment: (1) inter-critical annealing (IA) (2)-(3) bainite isothermal transformation (BIT) (3)-(4) final cooling to room temperature

Mechanical Properties

Swift Model

Jacques et al. Acta Mat., 2007

$$\sigma_i = K_i\left(1 + \varepsilon_{0,i}\varepsilon\right)^{n_i}$$

$$\sigma = \sum_i \sigma_i V f_i$$

$$\sigma = \sigma_A + (\sigma_B - \sigma_A)\frac{w_C^\gamma - 1.25}{0.25}$$

Composition and micro-structure in tensile tests

w_C		w_{Mn}		w_{Si}	
0.29		1.42		1.41	
	Vf_{Fer}	Vf_{Bai}	Vf_{Aus}	Vf_{Mar}	w_C^γ
A	55	28	17	0	1.25
B	55	33	12	0	1.5

	Phase	K_i, MPa	$\varepsilon_{0,i}$	n_i
A	Austenite	**720**	**62**	**0.3**
	BCC	**475**	**55**	**0.27**
	Martensite	**2000**	**800**	**0.005**
B	Austenite	**1130**	**80**	**0.2**
	BCC	**720**	**50**	**0.175**
	Martensite	**2000**	**800**	**0.005**

Optimum Heat Treatment for Fe-0.32C-1.42Mn-1.56Si

T_{IA}	T_{BIT}
943 - 1142	350 - 943

The temperature domains (Kelvin) for optimizing the heat treatment for **Fe-0.32C-1.42Mn-1.56Si**

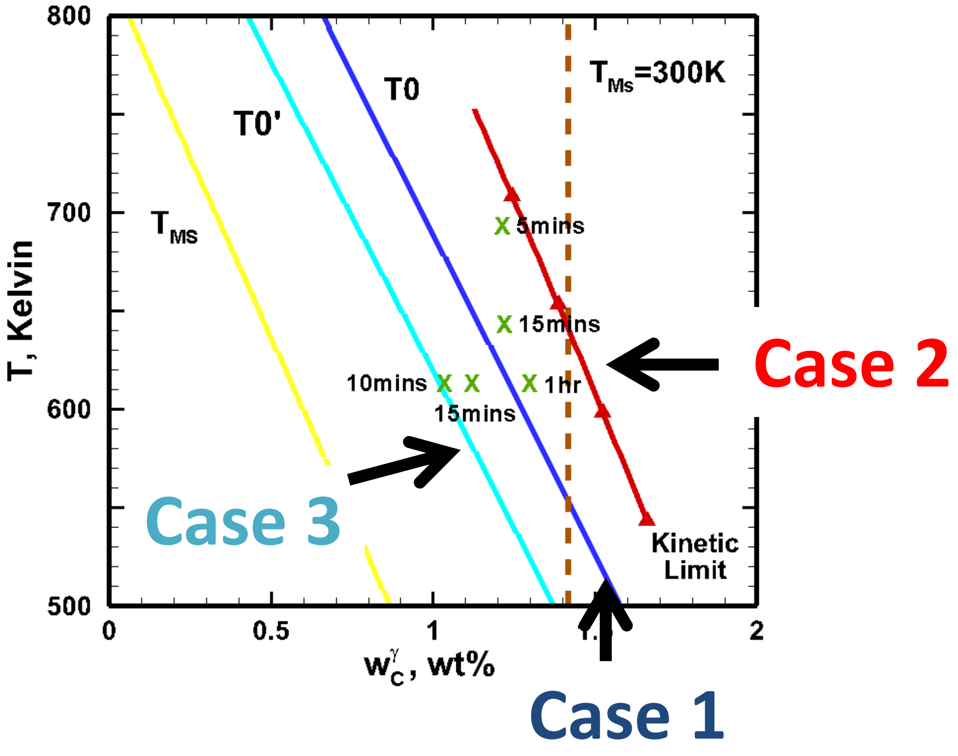

The Predictions for Case 1

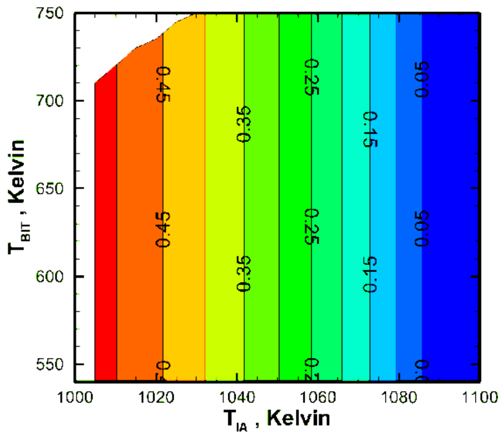

Vf(Fer)

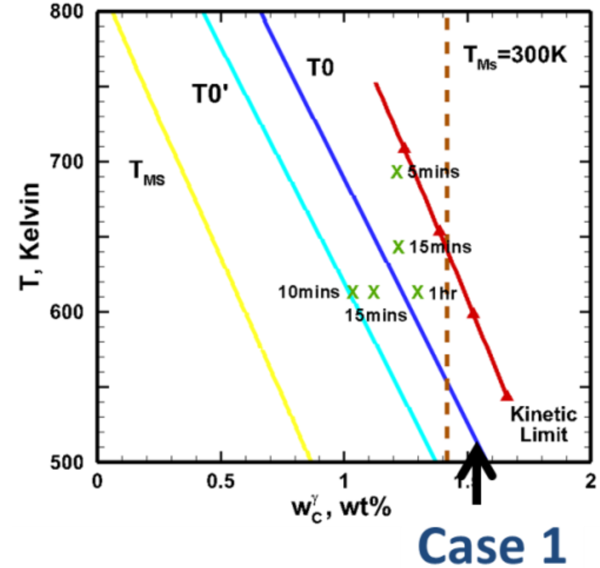

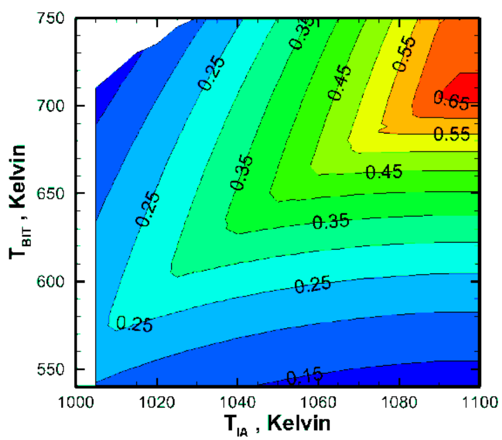

Vf(Bai)

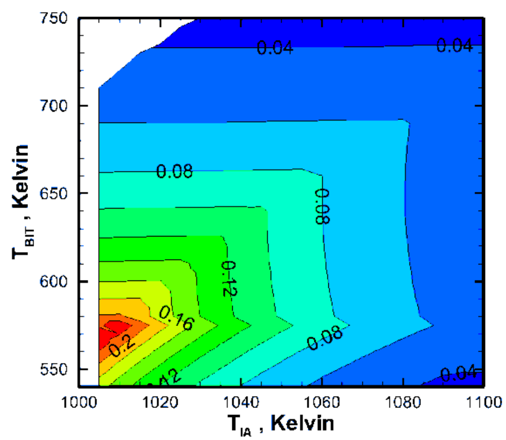

Vf(Aus)

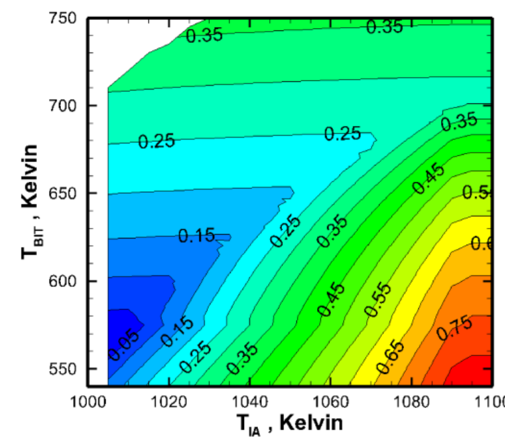

Vf(Mar)

The Predictions for Case 1

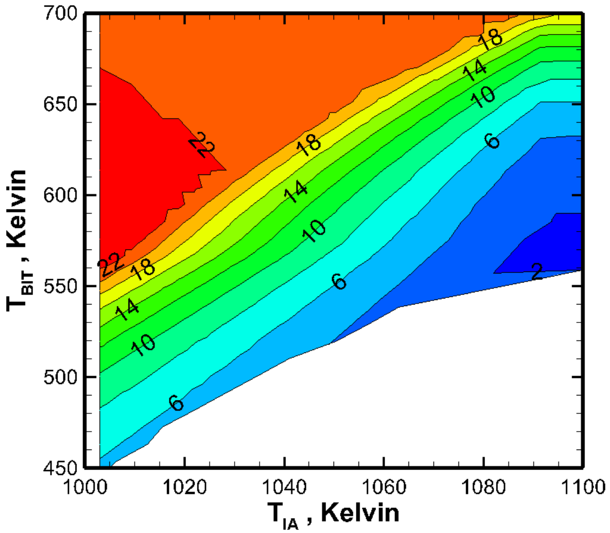

(1) Strain, %

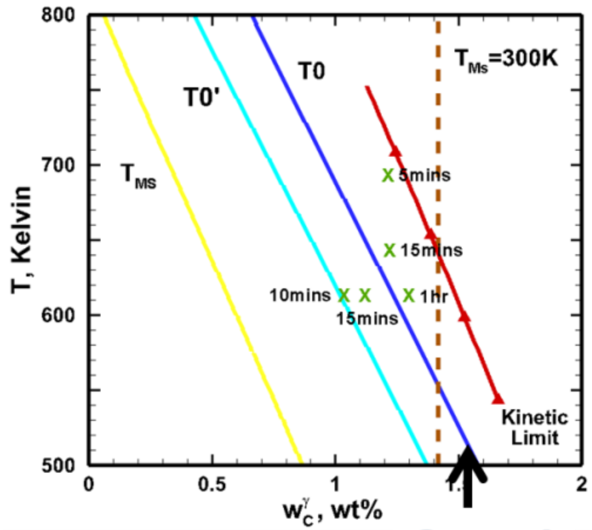

Case 1

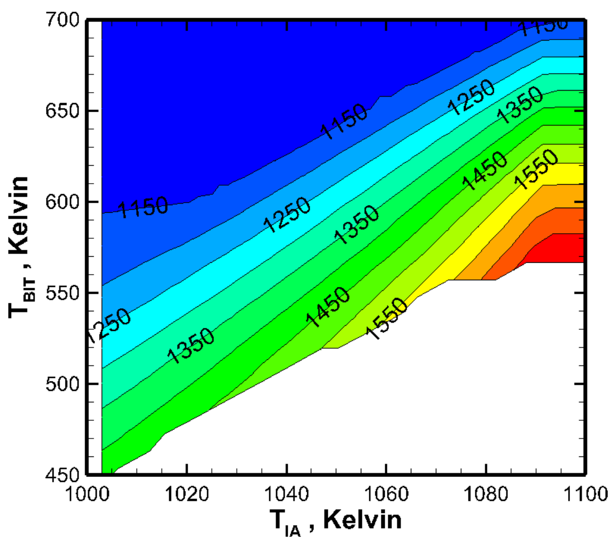

(2) Strength, MPa

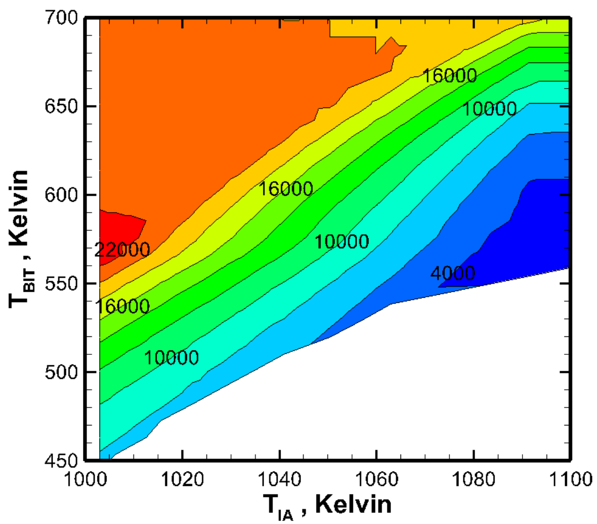

(3) WTN, MPa%

The Predictions for Case 2

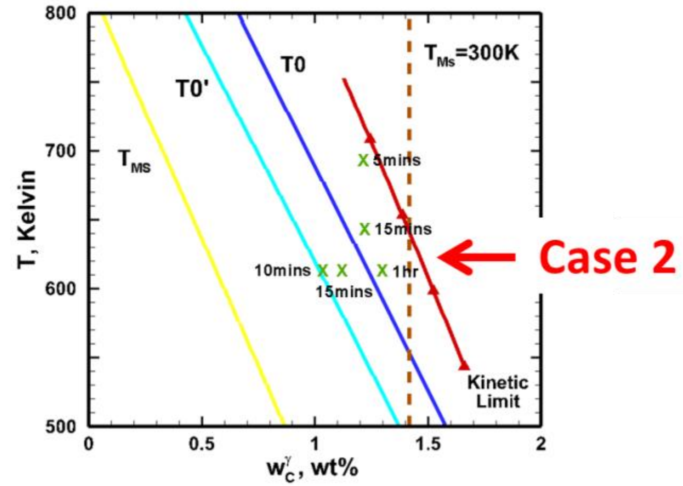

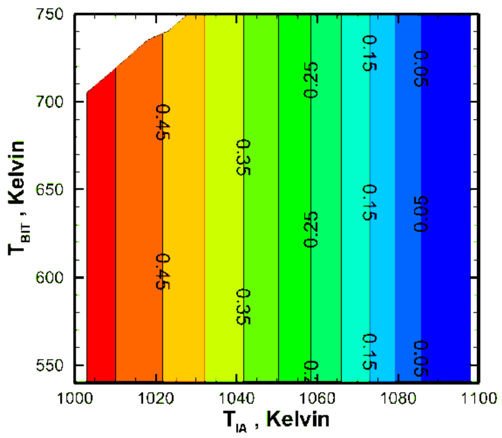

Vf(Fer)

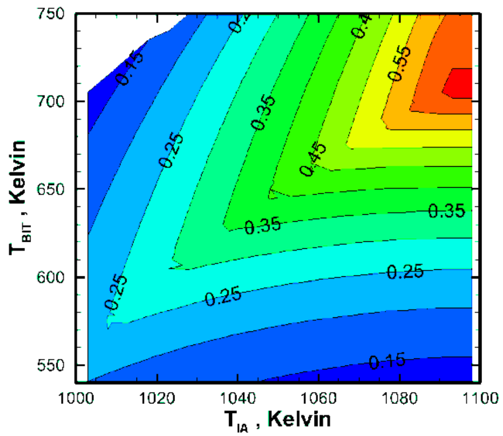

Vf(Bai)

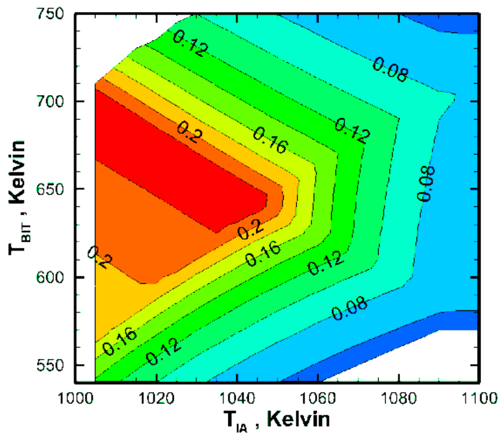

Vf(Aus)

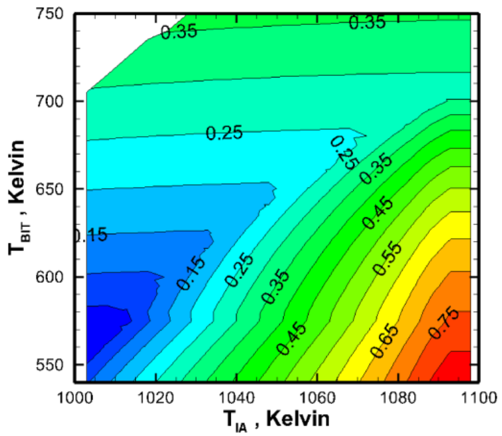

Vf(Mar)

The Predictions for Case 2

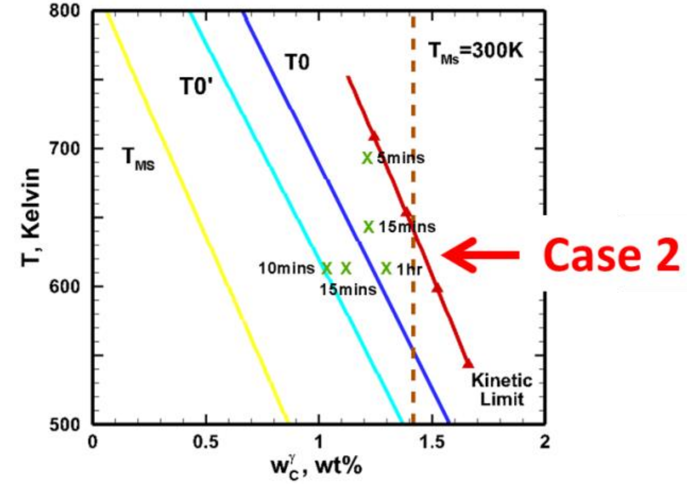

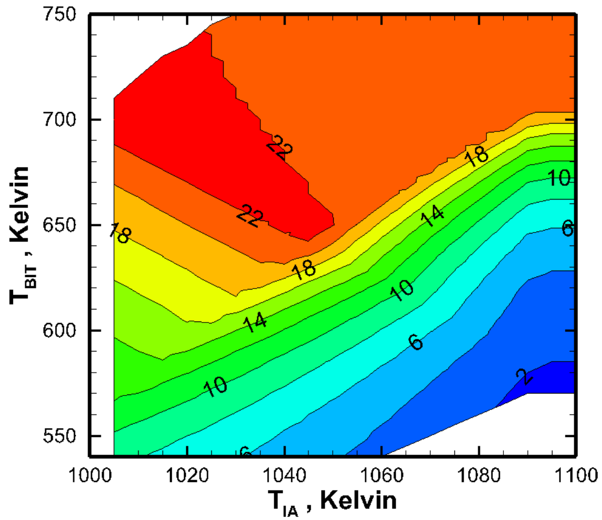

(1) Strain, %

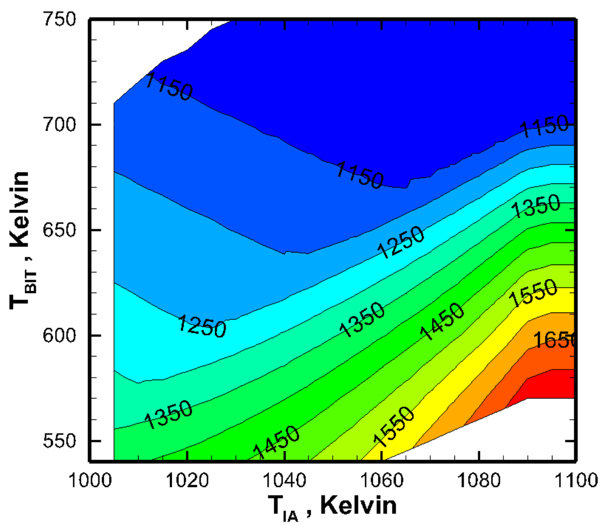

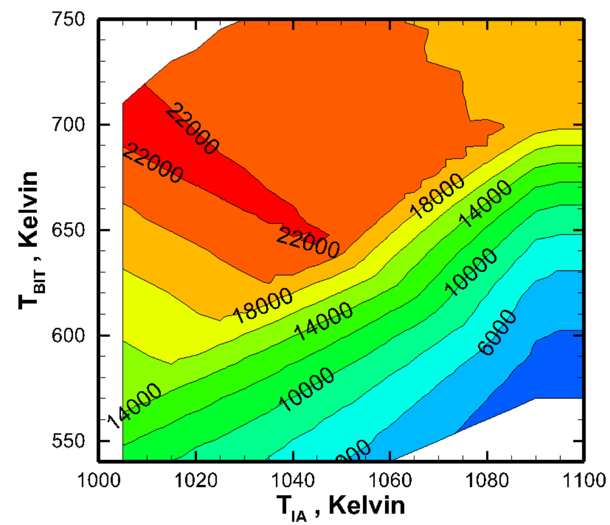

(2) Strength, MPa

(3) WTN, MPa%

The Predictions for Case 3

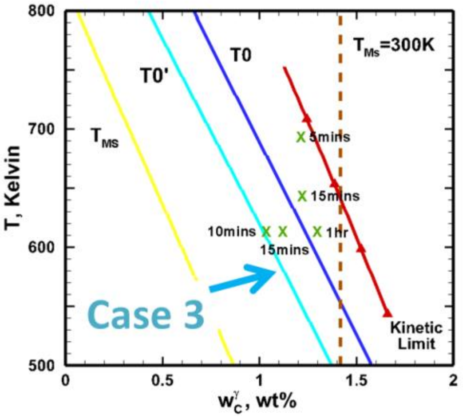

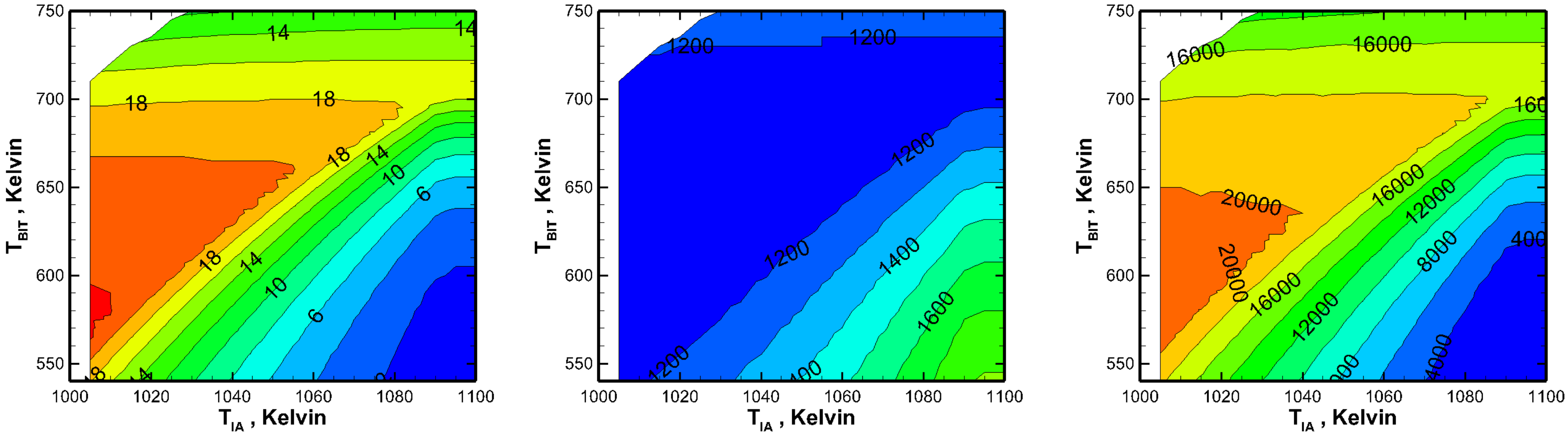

(1) Strain, %

(2) Strength, MPa

(3) WTN, MPa%

In T_0' calculations, for most of the microstructures the predicted retained austenite is less than 5%. Therefore, these diagrams include all the predicted microstructures.

Optimum Heat Treatment for Maximizing Toughness

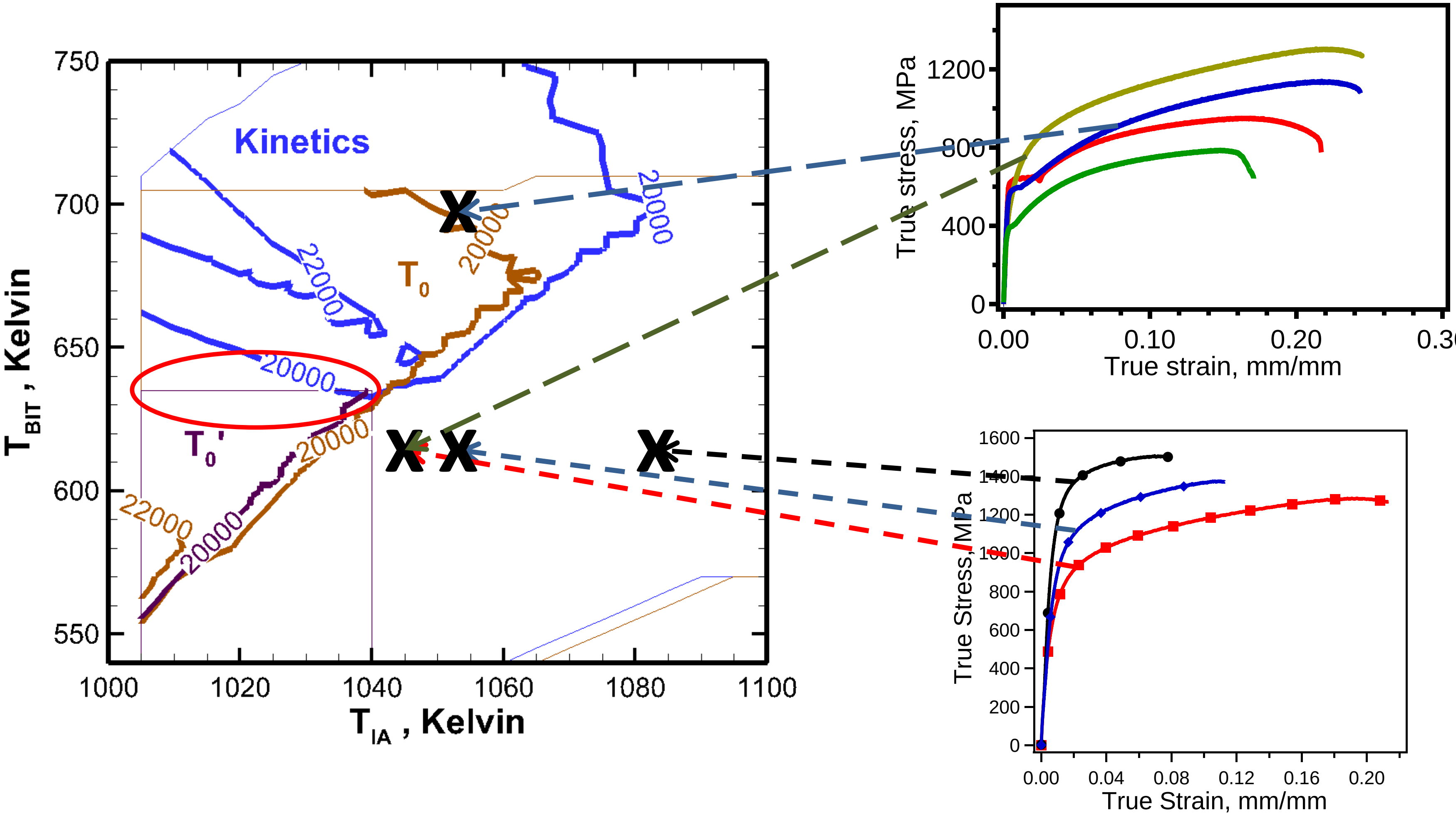

Experiments

Alloy Design Process

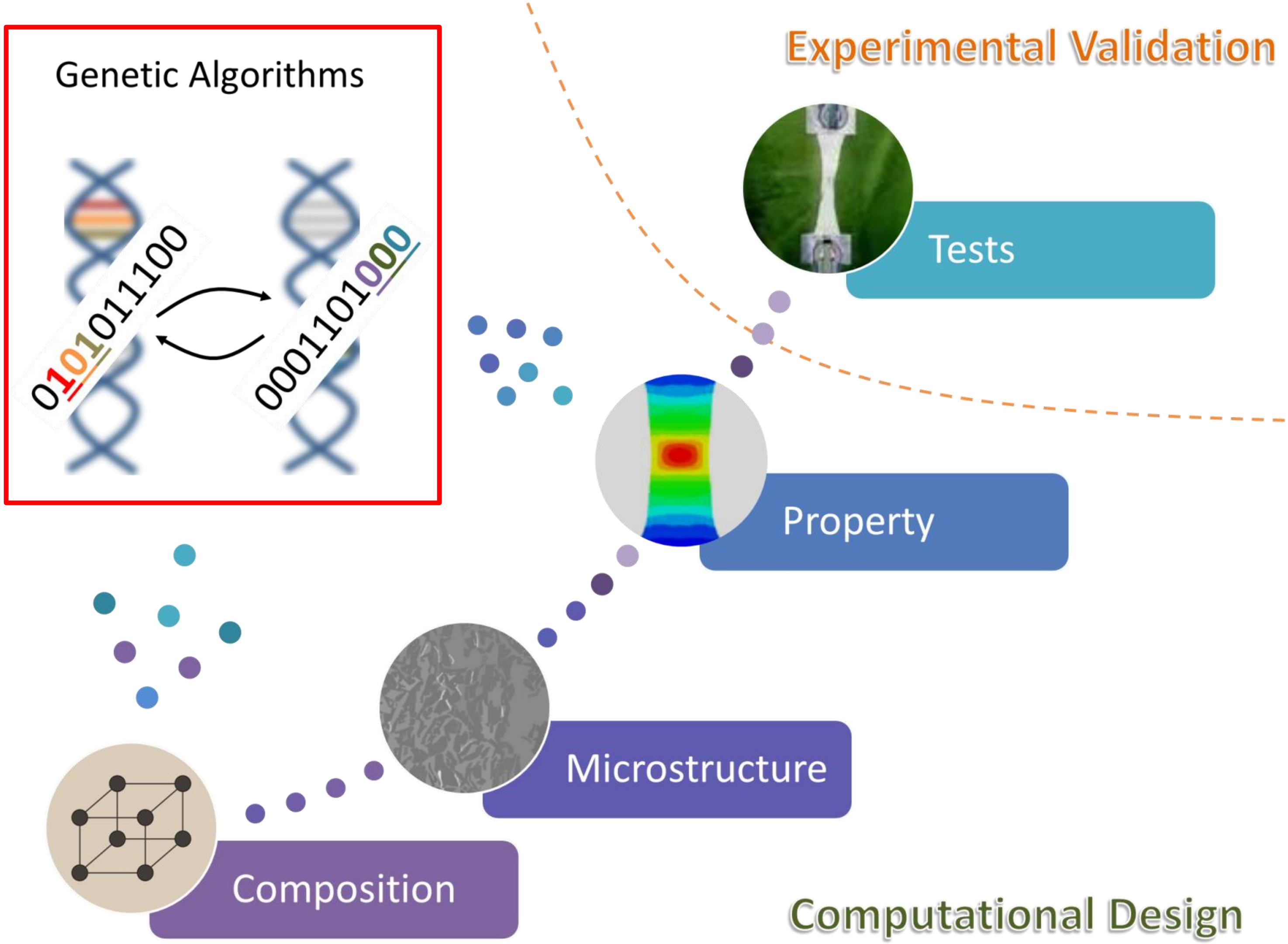

Genetic Algorithms - Schema

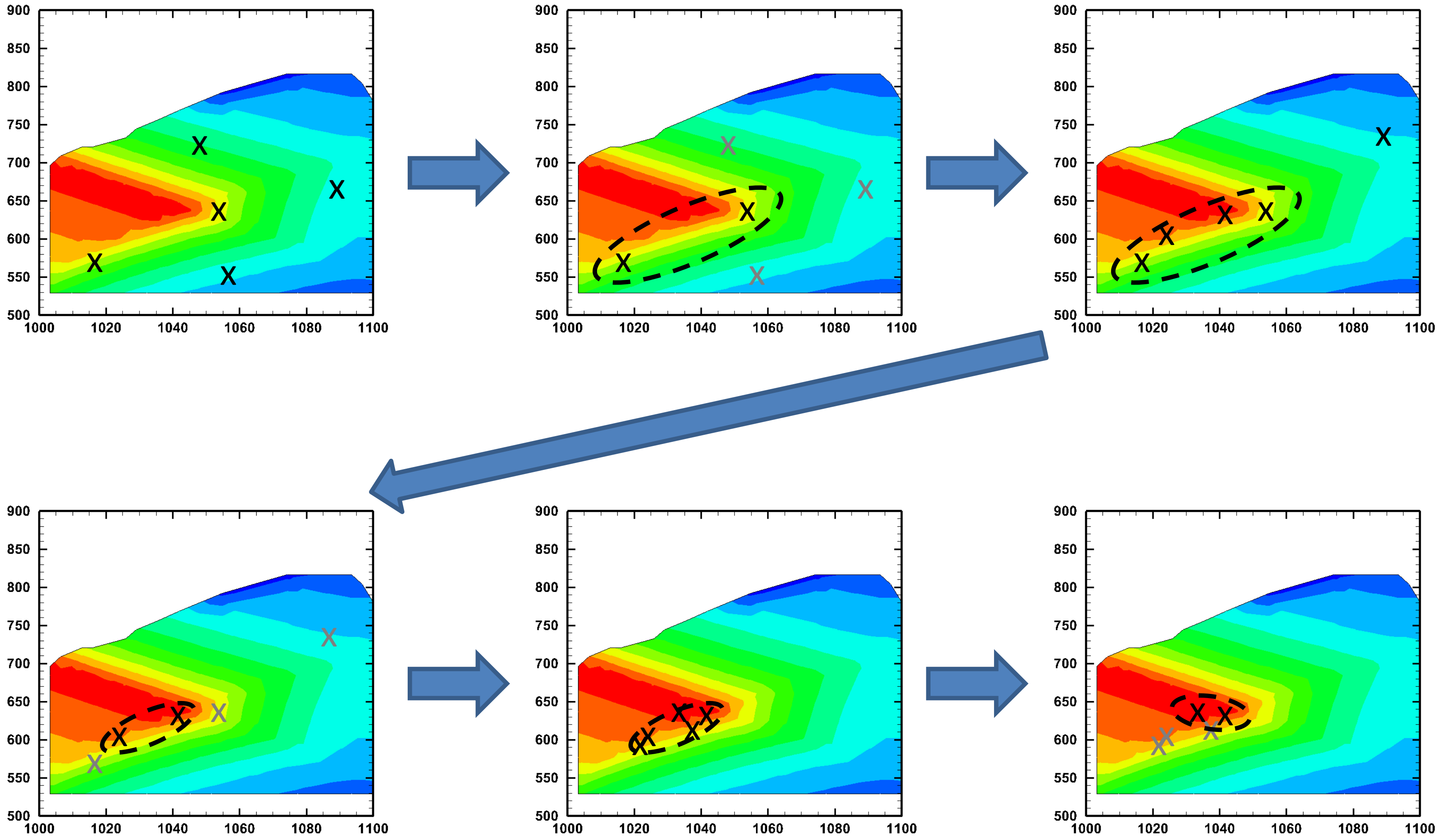

Optimum Composition and Heat Treatment

Composition, wt%; Temperature, Kelvin

w_C	w_{Mn}	w_{Si}
0.1 - 0.5	**0.5 - 2.5**	**0.8 - 1.5**

T_{IA}	T_{BIT}
943 - 1142	**350 - 943**

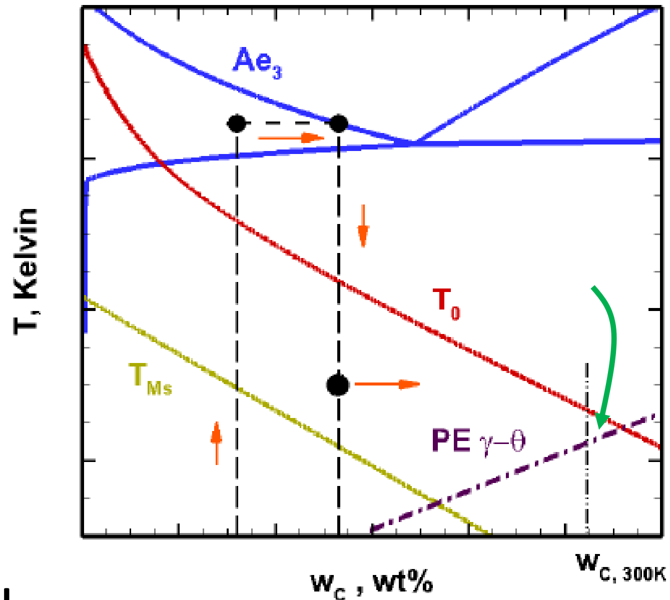

1. 6 bits memory for each variable
2. Vf_{Aus} > 5%
3. Total alloying addition is less than 4 wt%
4. 10 individuals in one generation, 1,000 generations
5. Full equilibrium after IA treatment is considered
6. T_0 and para $\gamma - \theta$ concepts are utilized

The Predicted Fitness as Function of Mechanical Properties

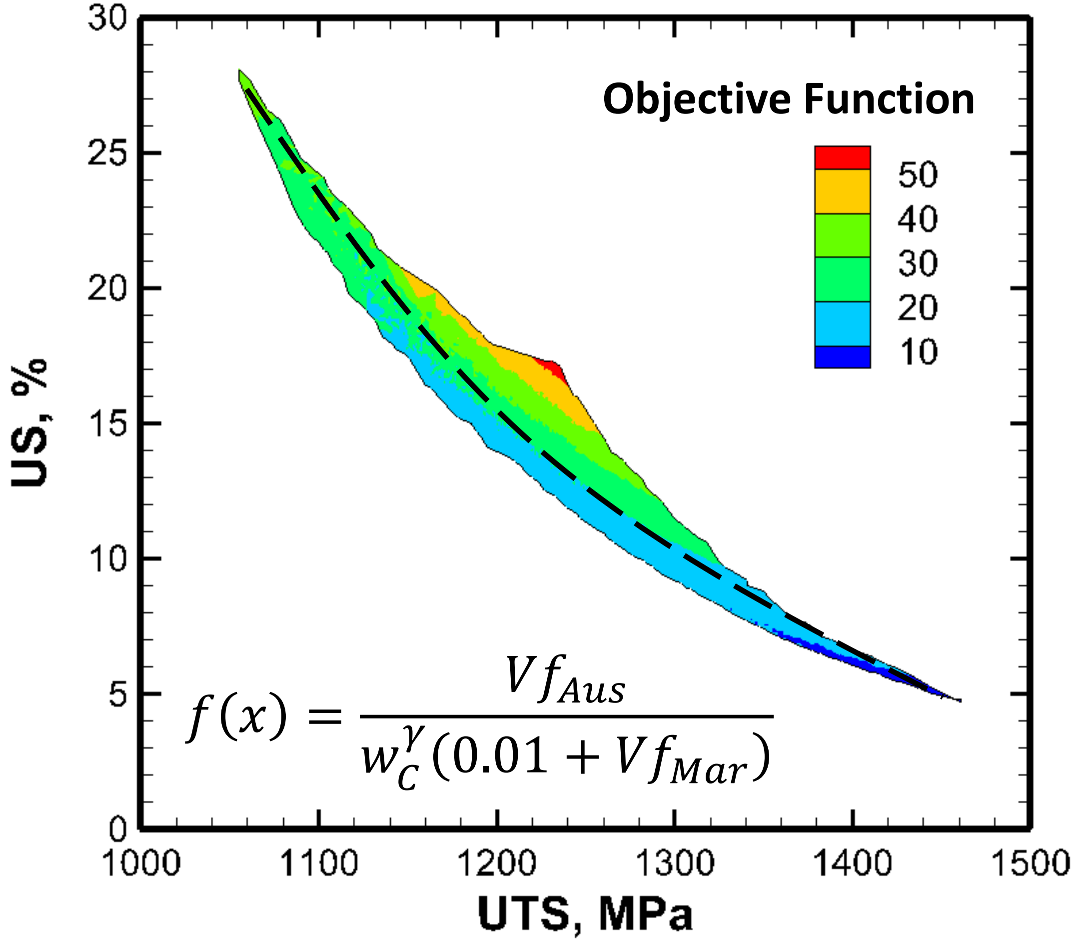

$$f(x) = \frac{Vf_{Aus}}{w_C^{\gamma}(0.01 + Vf_{Mar})}$$

Chemical Composition vs Mechanical Properties

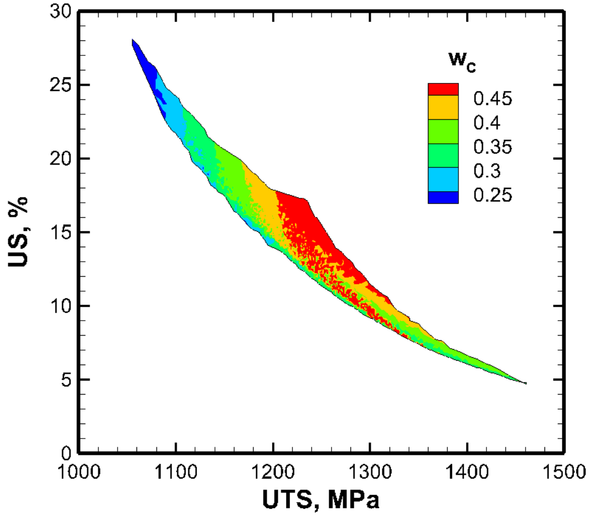

(1) w_C

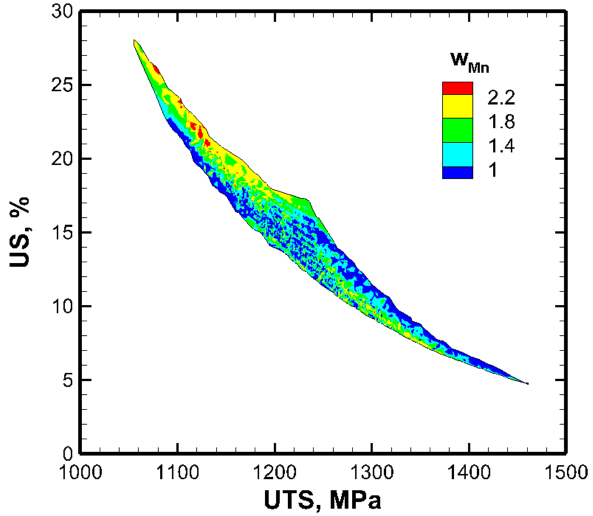

(2) w_{Mn}

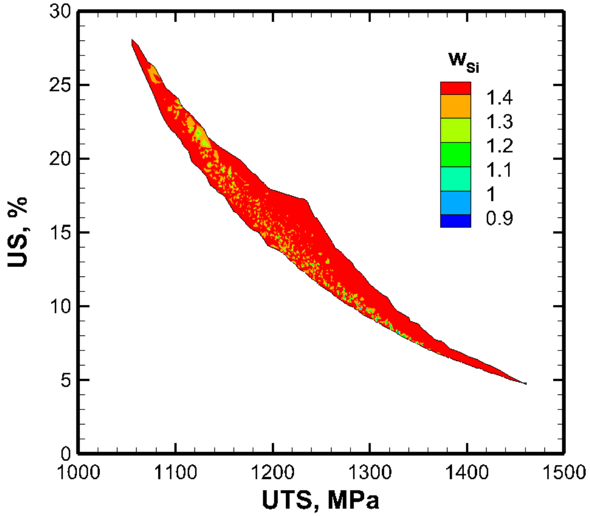

(3) w_{Si}

Fe-0.32C-1.42Mn-XSi

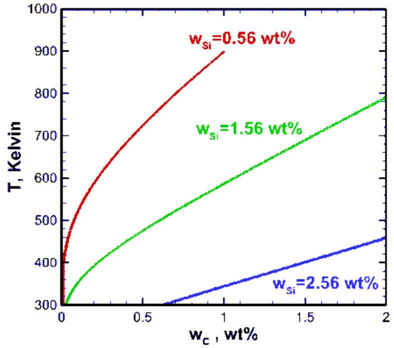

The Search in 6 Components, 2 Temperatures Domain

w_C	w_{Mn}	w_{Si}	w_{Al}
0.1 - 0.5	0.5 - 2.5	0.8 - 1.5	0.0 - 2.0
w_{Cr}	w_{Ni}	T_{IA}	T_{BIT}
0.0 - 1.33	0.0 - 2.0	943 - 1142	350 - 943

Composition, wt%; Temperature, Kelvin

1. 6 bits memory for each variable
2. Vf_{Aus} > 5%
3. Total alloying addition is less than 4 wt%
4. 10 individuals in one generation, 10,000 generations
5. Full equilibrium after IA treatment is considered
6. **T_0** and **para** $\boldsymbol{\gamma - \theta}$ concepts are utilized

Predicted Fitness as Function of Mechanical Properties

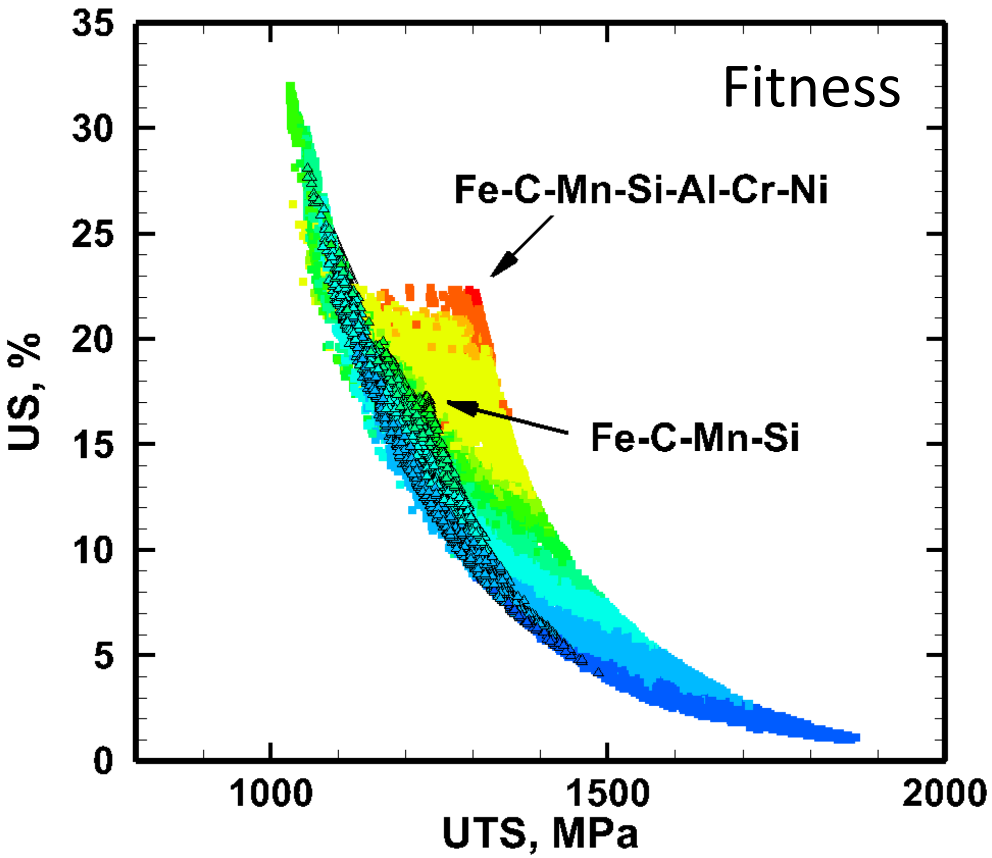

w_C	w_{Mn}	w_{Si}	w_{Al}
0.50	1.20	1.42	0.76
w_{Cr}	w_{Ni}	T_{IA}	T_{BIT}
0.04	0.00	1044	575

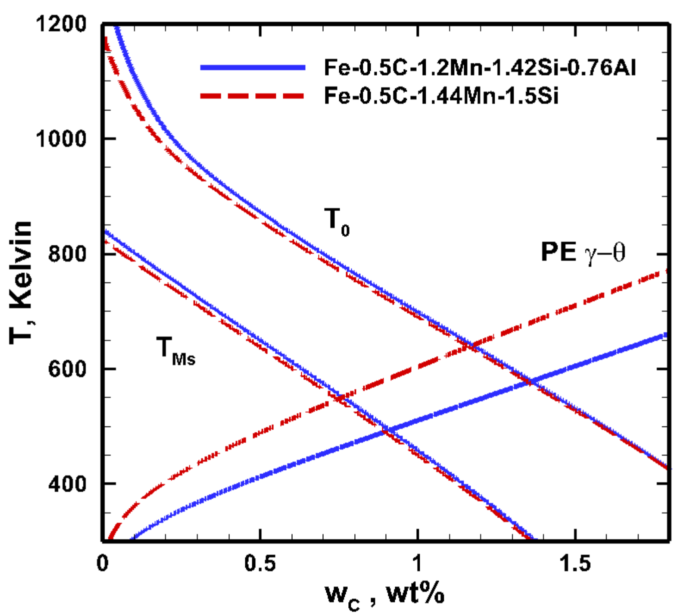

The predicted mechanical properties of Fe-C-Mn-Si-Al-Cr-Ni and Fe-C-Mn-Si alloys

Summary

CALPHAD Method

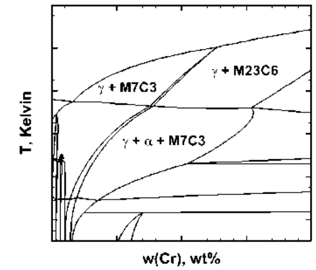

Composition Selection

C	Mn	Si	Al	Ni	Cr

Genetic Algorithm

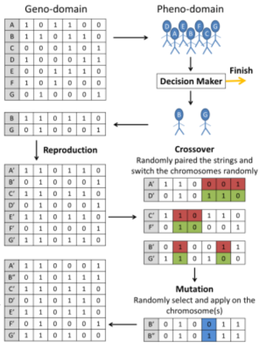

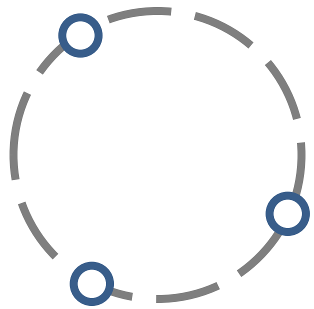

Micro-Structure

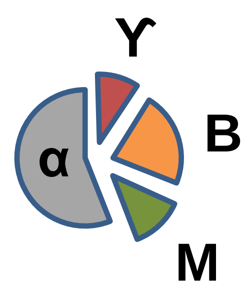

Mechanical Properties

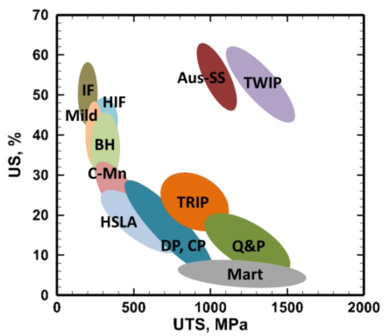

Mechanical Model based on Irreversible Thermodynamics

Swift Model

Plastic Deformation Model

Huang et al., 2008

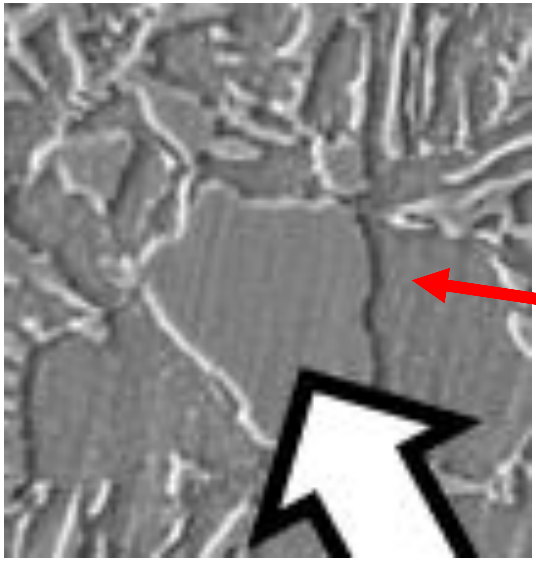

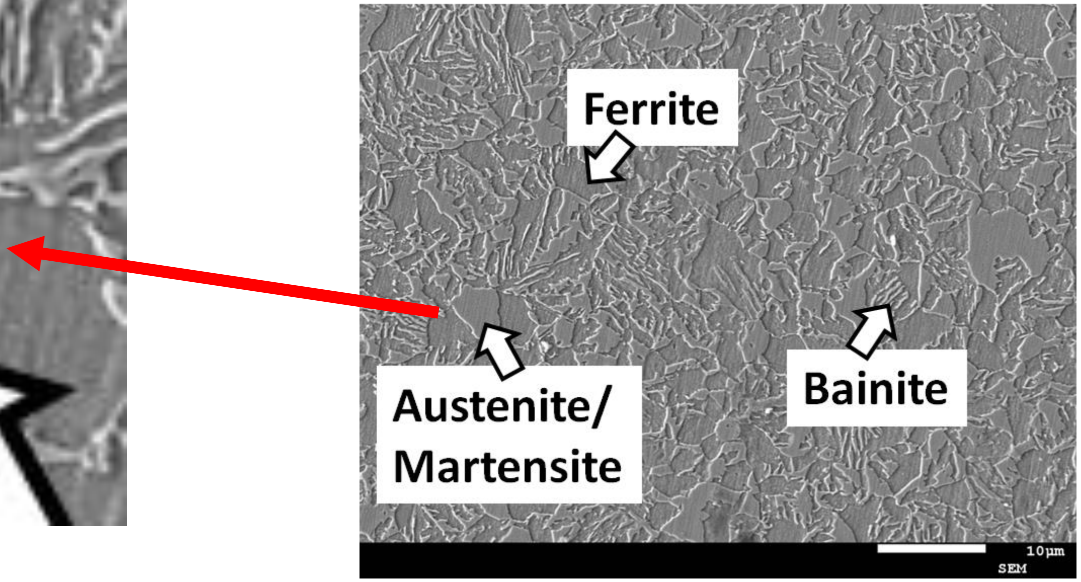

During the isothermal plastic deformation, the energy dissipation, dE can be attributed to (1) **the exchange of the energy with the environment, dQ;** (2) **energy consumption by dislocation variation, dW_E**

$$dE = TdS = \frac{Cb}{l} d\tau = dQ + dW_E$$

Plastic Deformation Model – cont. 1

- By energy conservation, dQ can be calculated

$$dQ = dU - dW_M$$

- Because of the dislocation: (1) **Generation, $\boldsymbol{dW_{ge}}$**; (2) **Glide, d$\boldsymbol{W_{gl}}$**; (3) **Annihilation, $\boldsymbol{dW_{an}}$**

$$dW_E = W_{ge} + W_{gl} + W_{an}$$

The energy dissipation can be estimated as:

$$dE = \frac{1}{2}\mu b^2 d\rho_{in}^{+} + \tau bld\rho_{in}^{+} + \frac{1}{2}\mu b^2 d\rho_{in}^{-} + \frac{1}{2}\mu b^2 d\rho_{in} - \tau_{in} d\varepsilon$$

Plastic Deformation Model – cont. 2

To estimate the shear stress (τ), several mechanisms are taken into account:

$$\tau = \tau_0 + \tau_s + \tau_{H-P} + \sqrt{\tau_{in}^2 + \tau_p^2}$$

τ_0: Peierls force [Irvine1969; Varin1988; Zhao 2007]

τ_s: solid-solution strengthening [Irvine1969; Varin1988; Zhao 2007]

τ_{H-P}: Hall-Petch effect [Irvine1969; Varin1988; Zhao 2007]

τ_{in}: dislocation strengthening inside the grain

τ_p: precipitation strengthening

Plastic Deformation Model – cont. 3

Huang et al., 2008

This energy dissipation is also related to (1) the hardness parameter (σ^*), (2) flow stress (τ), and (3) strain rate ($\dot{\gamma}$). It is proposed:

$$TdS = \frac{Cb}{l}d\tau$$

$$= \frac{1}{2}\mu b^2 d\rho_{in}^{+} + \tau bld\rho_{in}^{+} + \frac{1}{2}\mu b^2 d\rho_{in}^{-} + \frac{1}{2}\mu b^2 d\rho_{in} - \tau_{in}d\varepsilon$$

$$d\rho_{in} = d\rho_{in}^{+} - d\rho_{in}^{-}$$

$$d\rho_{in}^{-} = \frac{\nu_0}{\dot{\gamma}} exp\left(-\frac{\Delta G}{kT}\right)\rho_{in}d\gamma$$

Stress-Strain Curves of Steel Alloys

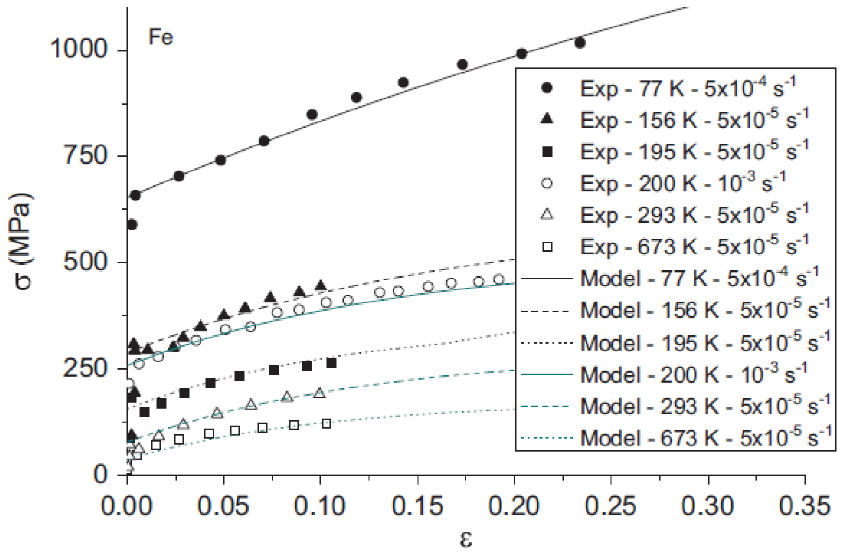

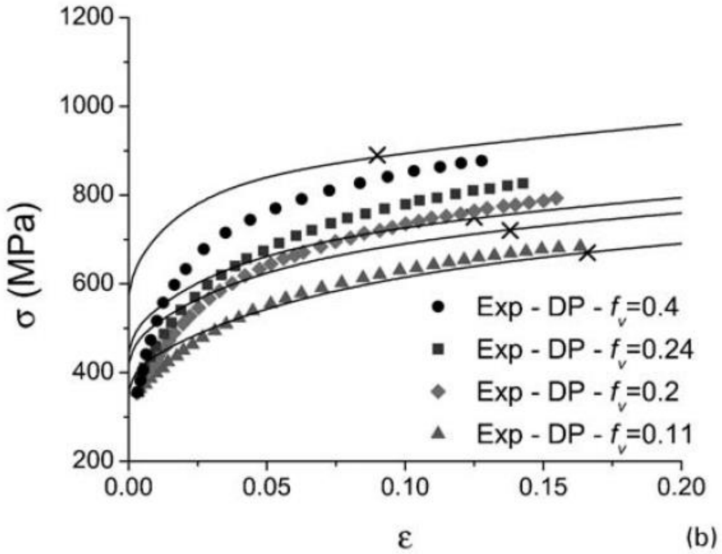

Ferrite

El Galindo-Nava et al., Mat. Sci. Eng. A 2012

Ferrite + Martensite

PEJ Rivera et al., Mat. Sci. Tech. 2012

Micro-Structure & Plastic Deformation

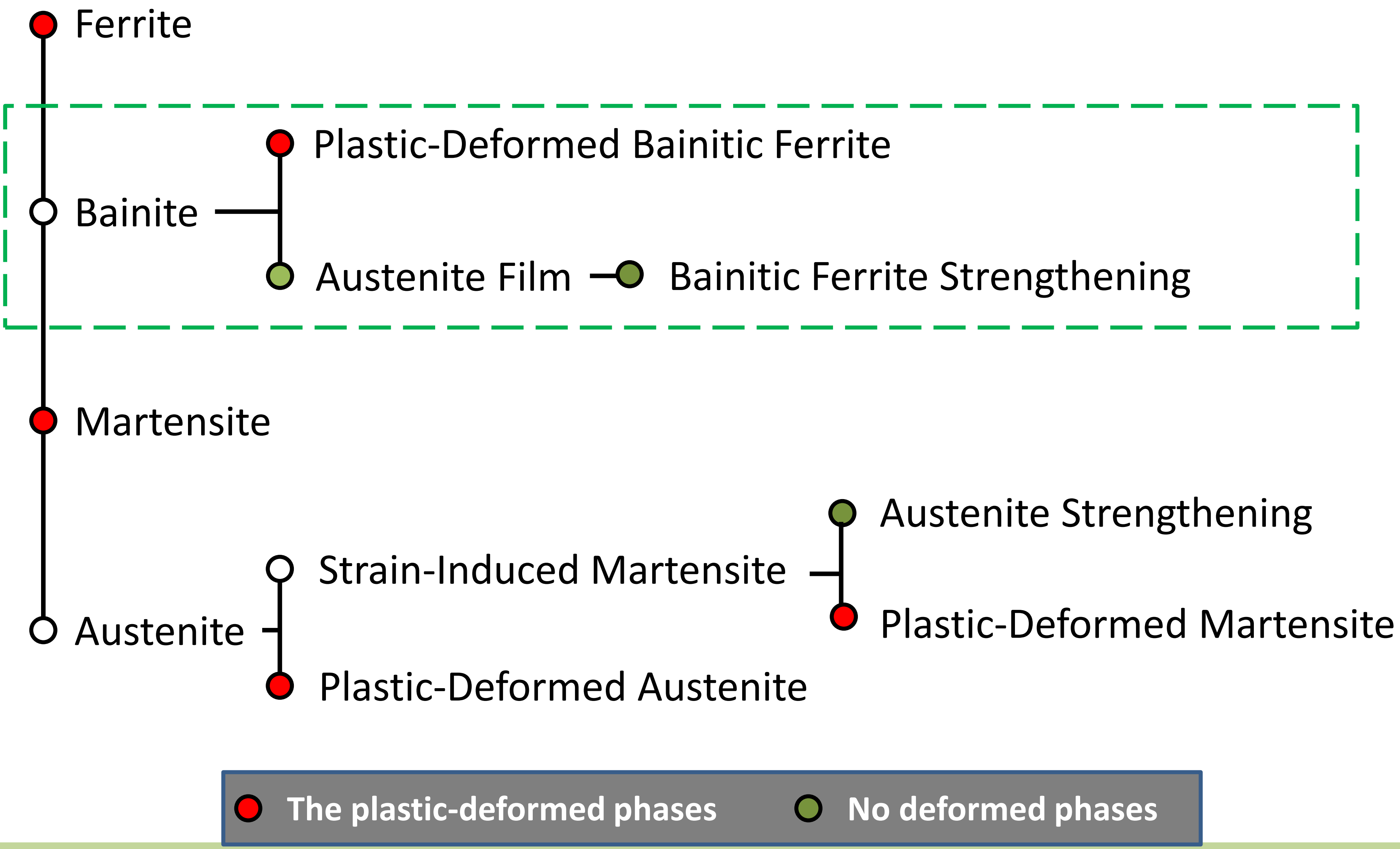

Bainite Sub-Unit Size

Garcia-Mateo et al., 2011

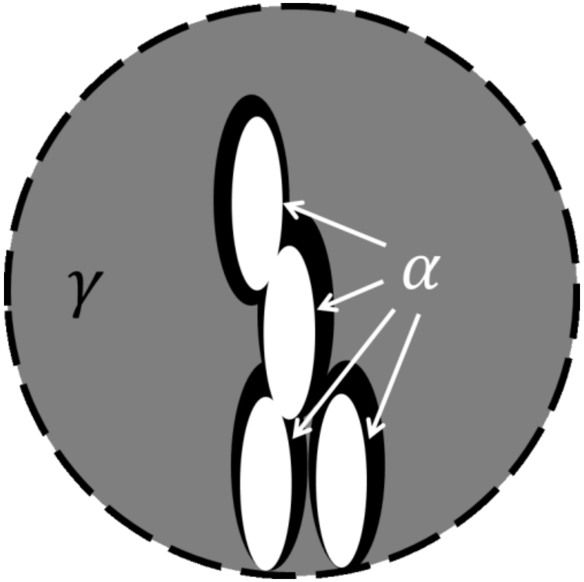

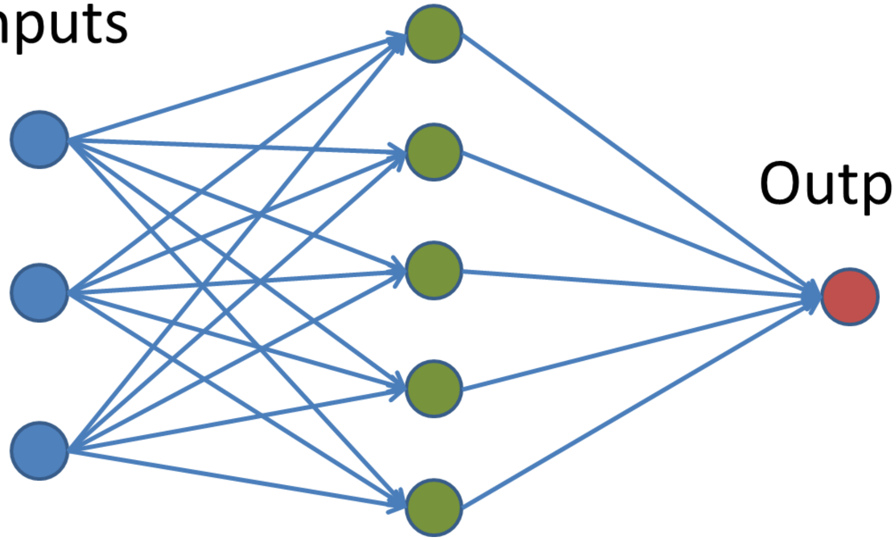

$$C_1 = \left(\sum x_n \omega_x\right) + \theta_1$$

$$H_1 = tanh(C_1)$$

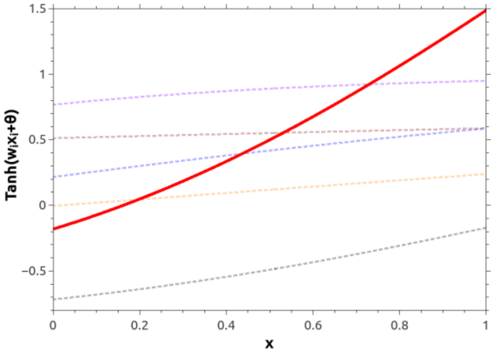

1. **Chemical Driving Force**
2. **Austenite Yield Strength**
3. **Temperature**

Mechanical Response of Bainite

Garcia-Mateo et al., 2011

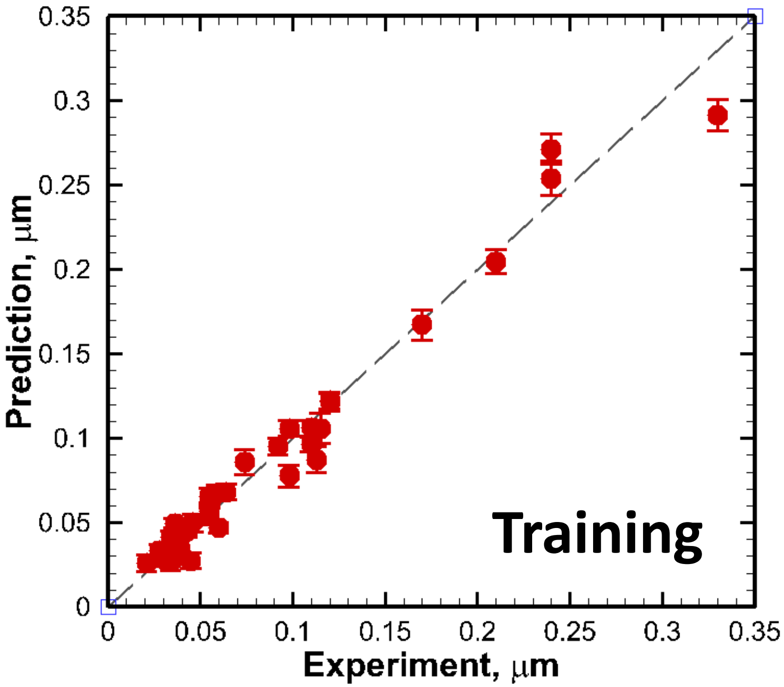

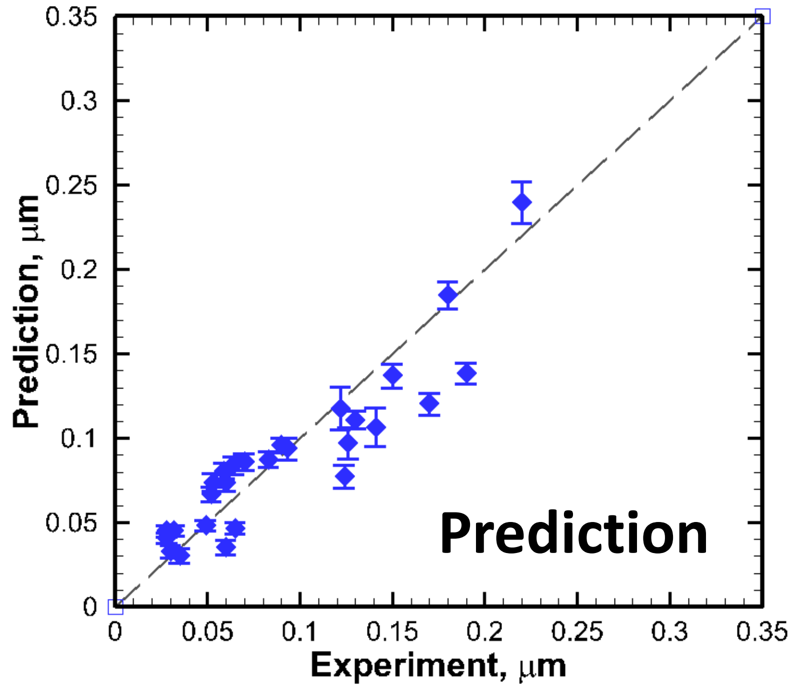

Micro-Structure & Plastic Deformation

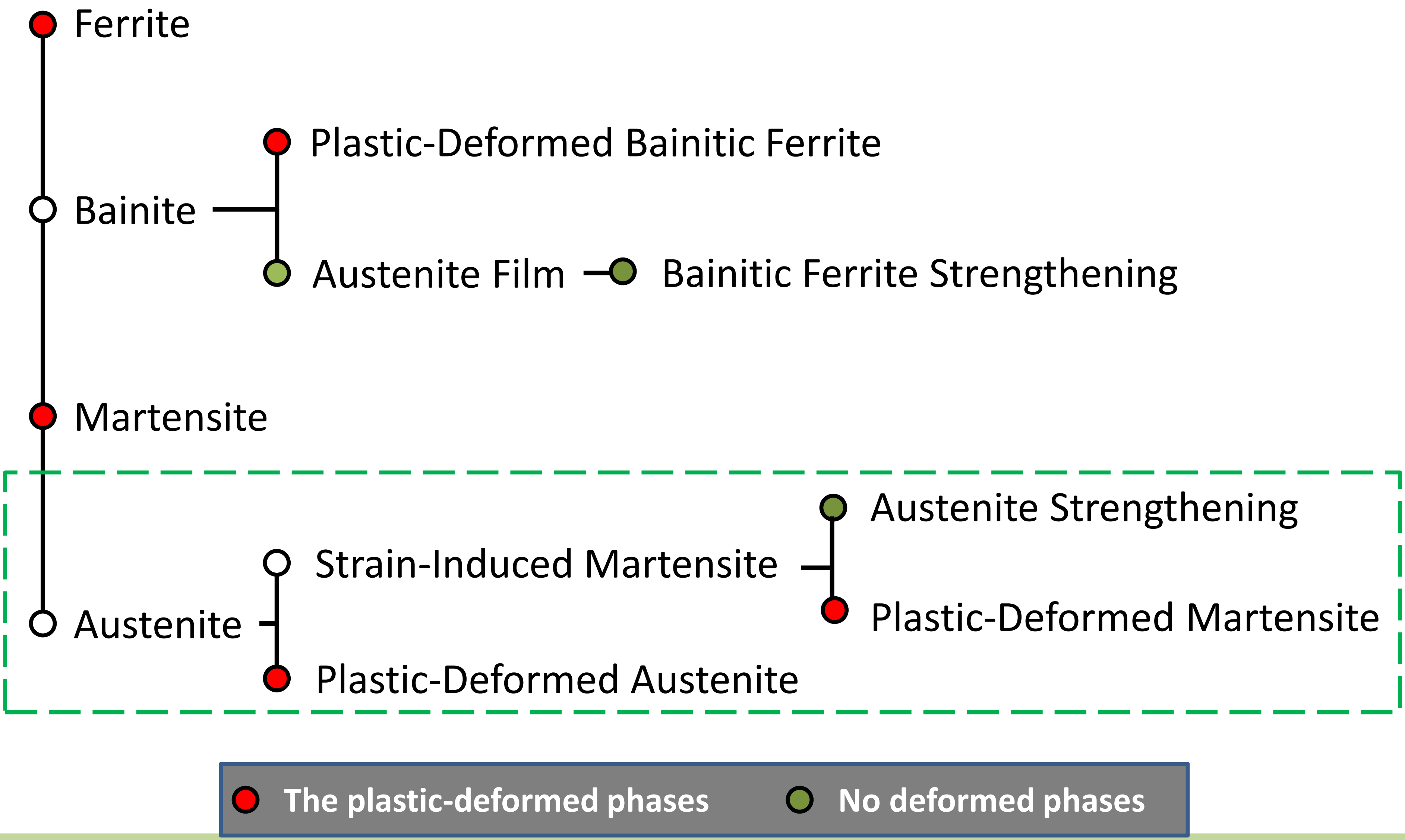

Parameters for Olson-Cohen Model

Olson et al., 1972, 1975

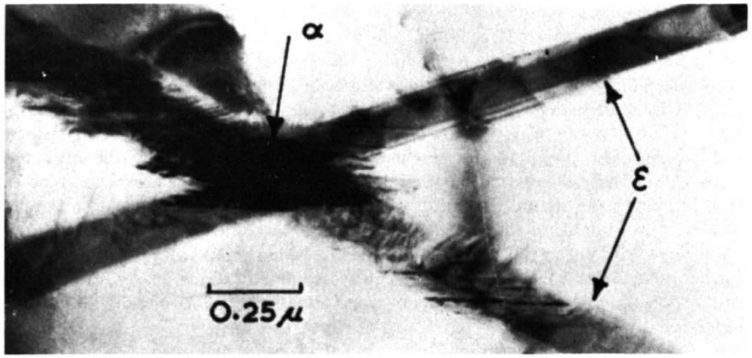

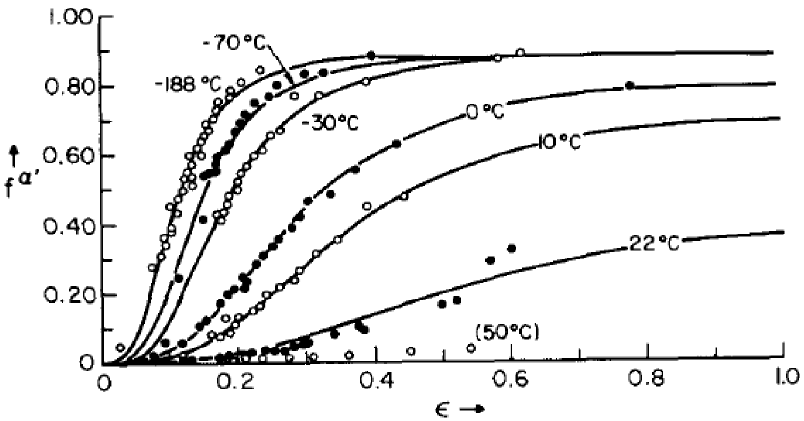

$$Vf_{\alpha'} = 1 - exp\left[-\beta\left(1 - exp(-\alpha\varepsilon)\right)^n\right]$$

Jacques et al., Phil. Mag. A, 2001

	Composition	O-C Param.
1	Fe-0.13C-1.42Mn-1.50Si	α=20, β=0.94
2		α=26, β=0.94
3		α=20, β=0.70
4	Fe-0.16C-1.30Mn-0.38Si	-
5		α=57, β=1.41
6		α=30, β=1.88
7		α=49, β=2.08
8		-

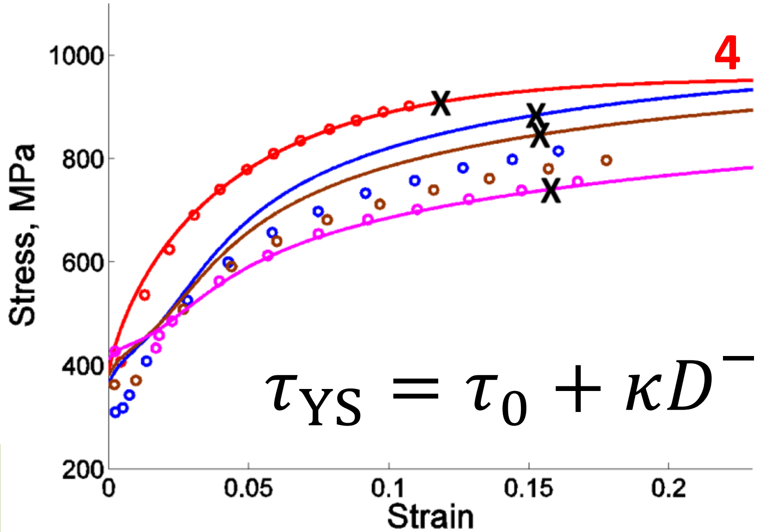

$$\tau_{YS} = \tau_0 + \kappa D^{-\frac{1}{2}}$$

Parameters for Olson-Cohen Model

$$Vf_{\alpha'} = 1 - exp\left[-\beta\left(1 - exp(-\alpha\varepsilon)\right)^{n}\right]$$

Jacques et al., Philosophical Magazine A, 2001

Strain Rate = 2 mm/min = 6.67E-4 s^{-1}

Composition	T_{BIT}, K	ΔG, J/mol	O-C Param.
Fe-0.13C-1.42Mn-1.50Si	683	-1785	α=20, β=0.94
	633	-2239	α=26, β=0.94
	683	-1860	α=20, β=0.70
Fe-0.16C-1.30Mn-0.38Si	-	-	-
	643	-2216	α=57, β=1.41
	643	-2216	α=30, β=1.88
	643	-2216	α=49, β=2.08
	643	-2216	-

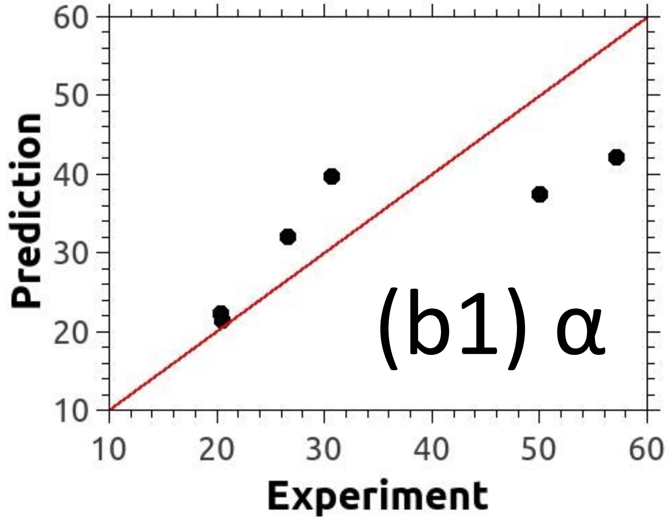

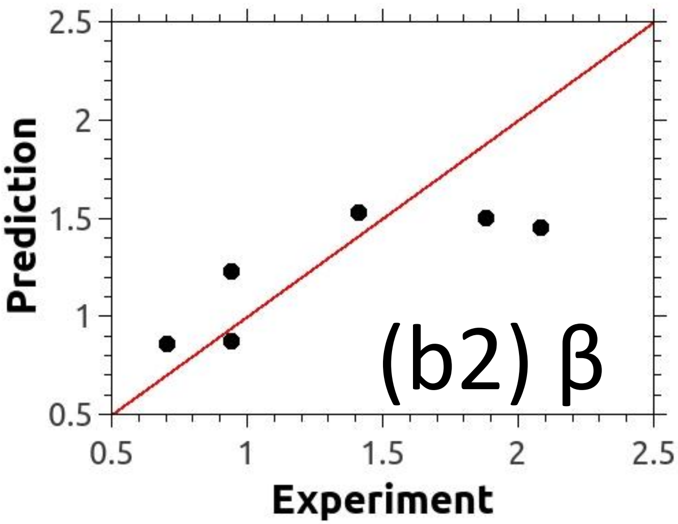

The Optimum Conditions for TRIP Steels

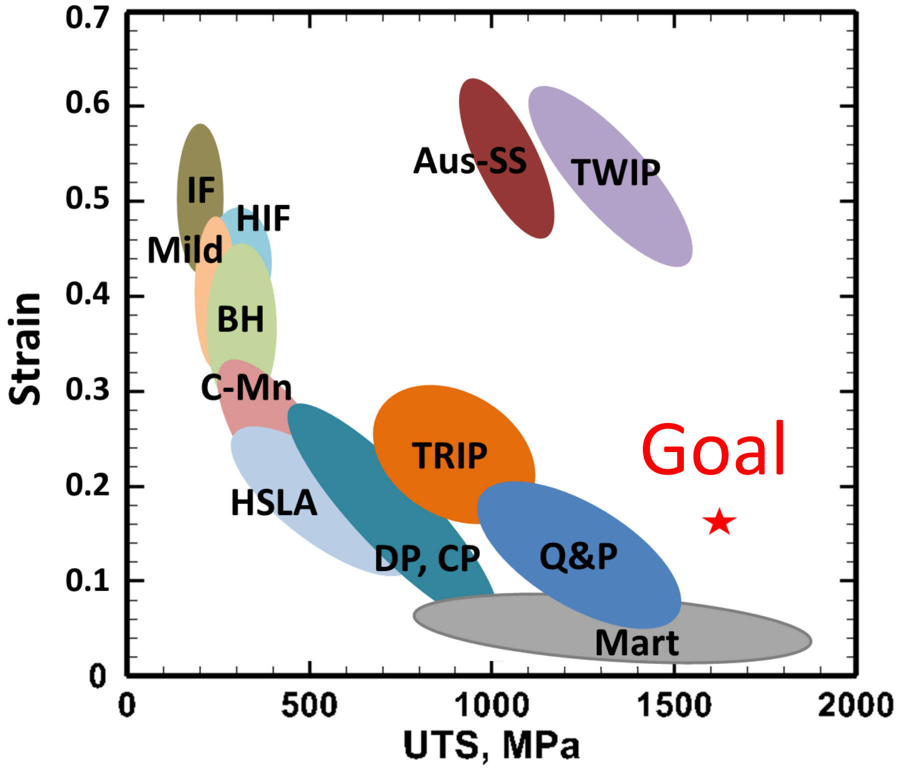

	C	Mn	Si	T_{IA}	T_{BIT}
Max	0.5	3.0	3.0	950	800
min	0.0	0.0	0.0	1100	500
MSize	$\mathbf{2^5}$			$\mathbf{2^7}$	

1. Total alloying addition is less than 4 wt%
2. 10 individuals in one generation, 1,000 generations
3. Full equilibrium after IA treatment is considered
4. **T_0** and **para** $\boldsymbol{\gamma - \theta}$ concepts are utilized

Phase Constituent and Performance

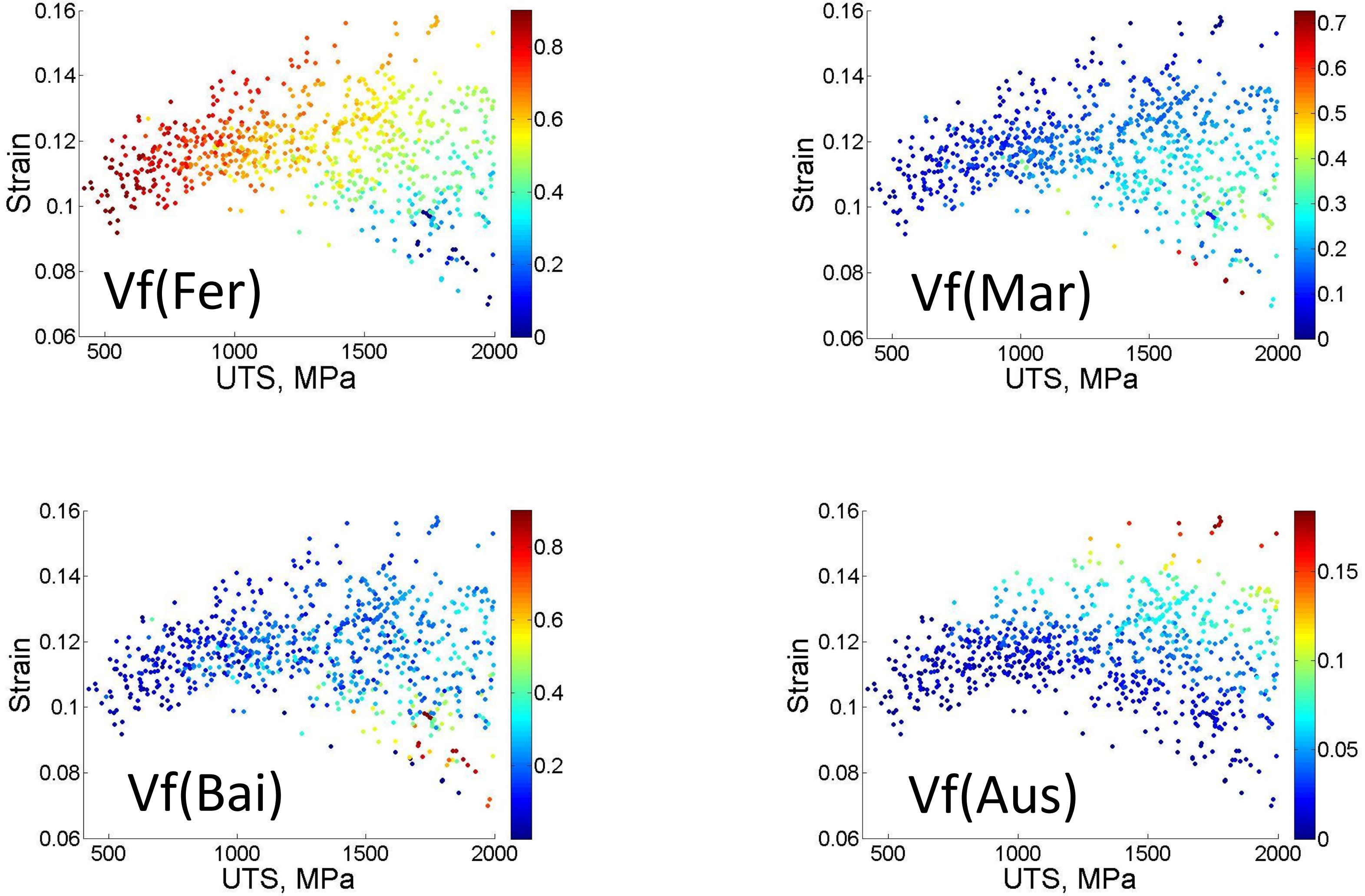

Chemical Composition and Performance

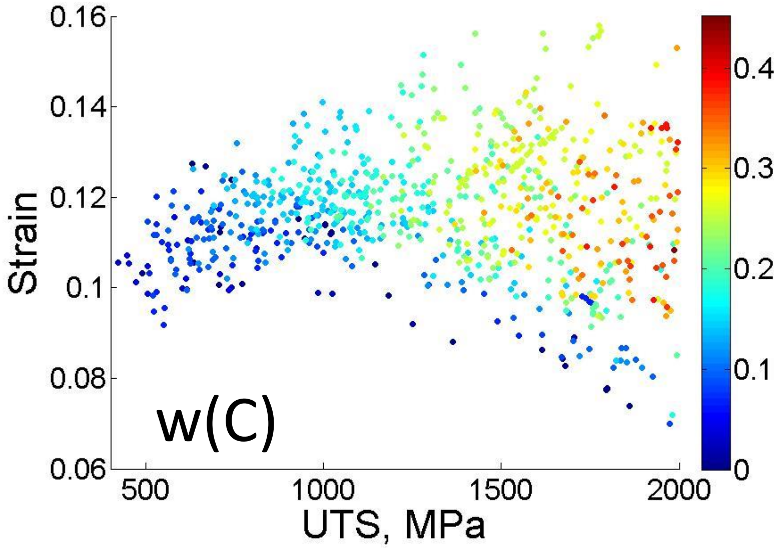

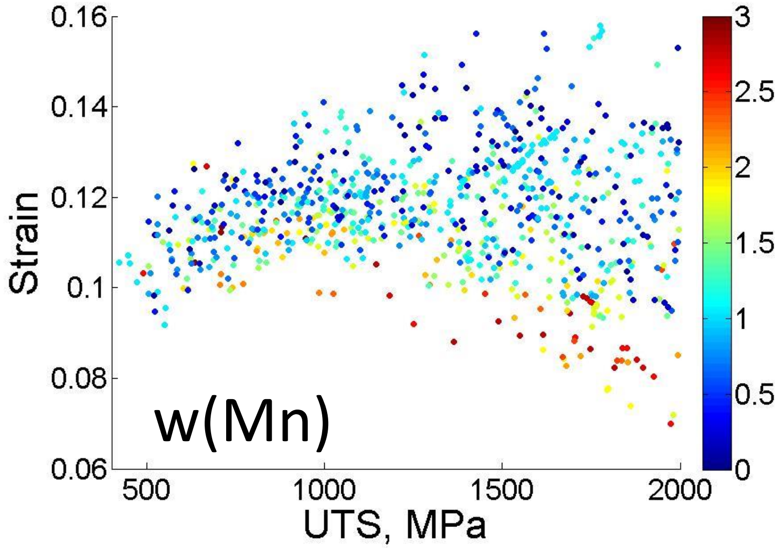

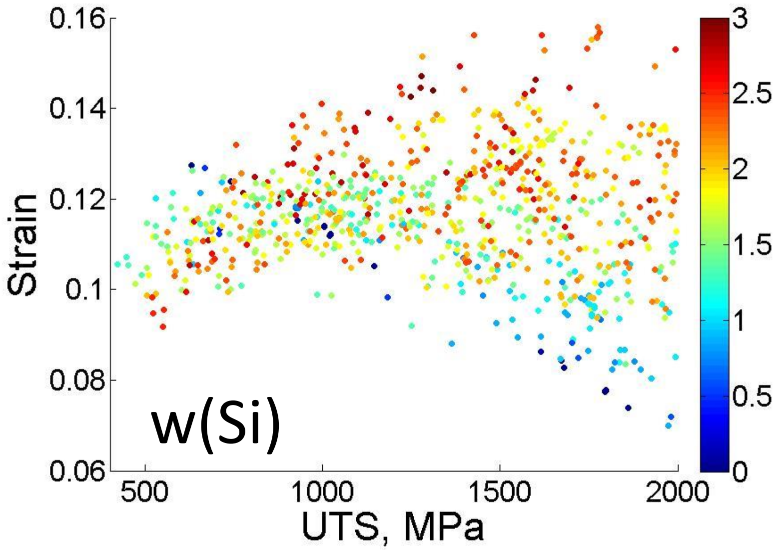

The Optimum Conditions

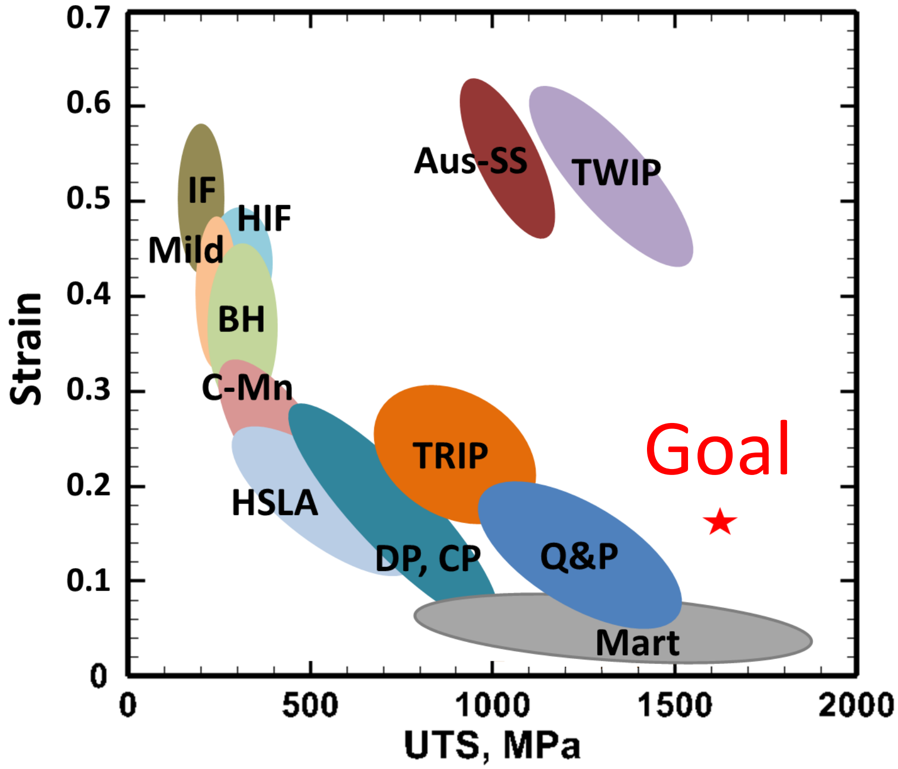

To achieve 15%-1600MPa, the recommended conditions are (wt%; K):

C	Mn	Si	T_{IA}	T_{BIT}
0.24	0.48	2.22	1051	601

Conclusion

Composition Selection

C	Mn	Si	Al

CALPHAD Method

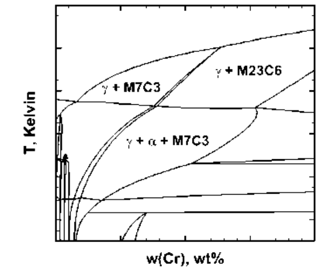

Genetic Algorithm

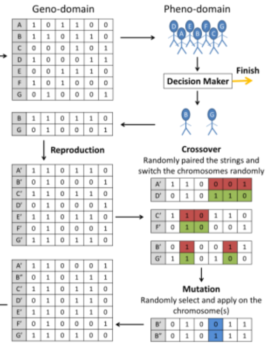

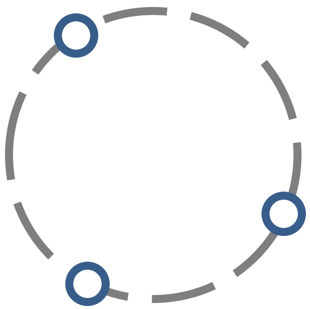

Micro-Structure

Mechanical Properties

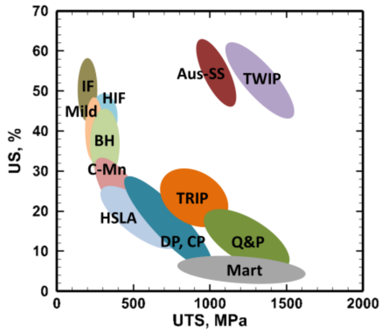

Mechanical Model based on Irreversible Thermodynamics

Selected References

1. S Li et al., Thermodynamic analysis of two-stage heat treatment in TRIP steels
2. S Li et al., Development of a Kinetic Model for Bainitic Isothermal Transformation in Transformation-Induced Plasticity Steels
3. H. Bhadeshia, Bainite in Steels.
4. Caballero et al., Design of Advanced Bainitic Steels by Optimisation of TTT Diagrams and T0 Curves
5. Xu et al., Genetic alloy design based on thermodynamics and kinetics
6. Matsumura et al., Mechanical properties and retained austenite in intercritically heat-treated bainite-transformed steel and their variation with Si and Mn additions
7. De Cooman, Structure–properties relationship in TRIPsteels containing carbide-free bainite
8. Fan et al., A Review of the Physical Metallurgy related to the Hot Press Forming of Advanced High Strength Steel